A Conditional Allele of the Novel Repeat-containing Yeast Nucleoporin *RAT7 / NUP159* Causes Both Rapid Cessation of mRNA Export and Reversible Clustering of Nuclear Pore Complexes

Lisa C. Gorsch, Thomas C. Dockendorff, and Charles N. Cole

Department of Biochemistry, Dartmouth Medical School, Hanover, New Hampshire 03755

Abstract. In a screen for *Saccharomyces cerevisiae* genes required for nucleocytoplasmic transport of messenger RNA, we identified the *RAT7* gene (ribonucleic acid trafficking), which encodes an essential protein of 1,460 amino acids. Rat7p is located at the nuclear rim in a punctate pattern characteristic of nucleoporins. Furthermore, the central third of Rat7p contains 22 XXFG and three XFXFG degenerate repeats that are similar to signature GLFG and XFXFG repeats present in a majority of yeast and some mammalian nucleoporins sequenced to date. Shift of a strain bearing the temperature-sensitive *rat7-1* allele from 23°C to 37°C resulted in rapid (within 15 minutes) cessation of mRNA export, but did not cause concomitant cytoplasmic accumulation of a reporter protein bearing a nuclear localization signal. This suggests that Rat7p may play a direct role in nucleocytoplasmic export of RNA. Immunofluorescence and thin section electron microscopy revealed that in *rat7-1* cells grown at 23°C, the majority of nuclear pore complexes (NPCs) were clustered on one side of the nucleus. No ultrastructural abnormalities of the nuclear envelope were seen. Interestingly, shifting *rat7-1* cells to 37°C for 1 h caused the NPCs to disperse, restoring near wild-type NPC distribution. After this temperature shift, the mutant Rat7p was no longer detectable by immunofluorescence.

NUCLEOCYTOPLASMIC export of messenger RNA is an essential step in eukaryotic gene expression. Although little is known about the movement of messages from their sites of transcription and processing within the nucleus to the nuclear periphery (for reviews see Maquat, 1991; Izzauralde and Mattaj, 1992; Elliott et al., 1994), it is well documented that mRNP particles consisting of mRNA and associated proteins exit the nucleus through nuclear pore complexes (NPCs)[1] embedded in the nuclear envelope. EM studies have shown that a well-characterized Balbiani ring mRNP particle formed in *Chironomus tentans* leaves the nucleus through NPCs (Stevens and Swift, 1966; Mehlin, et al., 1992). EM localization of RNA-coated gold particles microinjected into *Xenopus* oocyte nuclei demonstrated that poly(A)$^+$ RNA, tRNA, and 5S rRNA have the ability to direct export of gold particles through NPCs (Dworetzky and Feldherr, 1988). Recently, examination by EM of vertebrate cells subjected to in situ hybridization with digoxigenin-labeled oligo $dT_{(50)}$ followed by reaction with antidigoxigenin antibodies coupled to colloidal gold particles confirmed that endogenous poly(A)$^+$ RNA exits the nucleus through NPCs (Huang et al., 1994). Numerous other studies have demonstrated that proteins are imported into nuclei through NPCs (for reviews see Silver, 1991; Gerace, 1992). NPCs constitute the only known channels for exchange of macromolecules between the nucleus and cytoplasm.

The precise mechanisms of RNP translocation through the NPC are unknown. EM studies have shown that RNP particles associate with fibrous material extending into the nucleoplasm from the nuclear face of the NPC (Scheer et al., 1988; Mehlin et al., 1992). Presumably, this material constitutes a structure called the nuclear basket, which has been proposed to act as a guide for the movement of export substrates toward the NPC. Consistent with this, analysis of subnuclear poly(A)$^+$ RNA distribution in mammalian cells showed that areas of high concentration of poly(A)$^+$ RNA taper as they approach NPCs (Huang et al., 1994). The existence of one or more NPC-associated mRNP receptors is implied by the finding that Balbiani ring mRNP particles are always oriented in the same way at the pore entrance before translocation and proceed through the NPC in a directional

Address all correspondence to Charles N. Cole, Department of Biochemistry, Dartmouth Medical School, Hanover, NH 03755. Tel: (603) 650-1628. Fax: (603) 650-1128.

1. *Abbreviations used in this paper*: ABW, antibody wash; DAPI, 4,6-diamidino-2-phenylindole; GST, glutathione S-transferase; HA, hemagglutinin; IF, immunofluorescence; mD, megadaltons; mRNP, messenger RNP; NPC, nuclear pore complex; ORF, open reading frame; RAT, ribonucleic acid trafficking; ts, temperature sensitive; YPD, YPR, YPG, yeast extract, bactopeptone, and dextrose, raffinose, or galactose, respectively.

manner with the 5′ end of the particle in the lead (Mehlin et al., 1992). The very large diameter of these Balbiani ring RNP particles requires that they unfold as they pass through the NPC (Scheer et al., 1988; Mehlin et al., 1992).

NPCs span the nuclear envelope at sites where the inner and outer nuclear membranes are fused. NPCs are composed of ~100 distinct proteins and have an estimated molecular mass of 125 megadaltons (mD) in *Xenopus* and 65 mD in yeast (Reichelt et al., 1990; Rout and Blobel, 1993). The structure of the NPC is believed to be similar in all eukaryotic organisms (Maul, 1977) and has been determined using EM and high-resolution image reconstruction (Unwin and Milligan, 1982; Hinshaw et al., 1992; Akey and Radermacher, 1993). Briefly, the NPC is thought to consist of two coaxial rings that are coplanar with the inner and outer membranes of the NE and are connected by eight "spokes" that extend inward and delimit a central channel. The outermost region of the spokes are located within the lumen of the NE where, presumably, they serve to anchor the NPC in the pore membrane. Eight short fibrils emanate from the cytoplasmic ring into the cytoplasm. Eight longer fibrils protrude from the nuclear ring into the nucleoplasm, where their ends are connected by a smaller ring which forms the base of a basket-like structure (Jarnik and Aebi, 1991; Ris, 1991). There is evidence that NPCs are attached to the nuclear lamina via their nuclear rings (Stewart and Whytock, 1988; Akey, 1989) and to a separate "nuclear envelope lattice" via the distal basket ring (Goldberg and Allen, 1992).

At present, the sequences of only 8 vertebrate and 11 yeast NPC proteins (also called nucleoporins) are known (for review see Rout and Wente, 1994). Two nucleoporin subfamilies have been defined on the basis of highly repeated sequence motifs. Yeast Nup49p/Nsp49p, Nup100p, Nup116p/Nsp116p (Wente et al., 1992; Wimmer et al., 1992), and Nup145p (Fabre et al., 1994; Wente and Blobel, 1994) all contain GLFG (gly-leu-phe-gly) repeats, whereas degenerate XFXFG (X-phe-X-phe-gly) repeats exist in vertebrate p62 (Starr et al., 1990; Carmo-Fonseca et al., 1991; Cordes et al., 1991), Nup153p (Sukegawa and Blobel, 1993) and Pom121p (Hallberg et al., 1993), and in yeast Nup1p (Davis and Fink, 1990), Nsp1p (Hurt, 1988), and Nup2p (Loeb et al., 1993). The functional significance of these repeats is unclear, though in some cases they can be deleted (Nehrbass et al., 1990; Loeb et al., 1993) without affecting cell viability.

Individual yeast nucleoporins have been implicated in nucleocytoplasmic transport. Nup100p, Nup116p, and Nup145p all contain a novel RNA binding motif that has been shown to mediate binding to homopolymeric RNA in vitro, suggesting that these proteins could interact directly with RNA during its transport through the NPC (Fabre et al., 1994). Depletion of Nup145p from wild-type cells results in the gradual impairment of both poly(A)$^+$ RNA export and, somewhat later, protein import (Fabre et al., 1994). Yeast strains bearing various conditional alleles of *NUP1* also show defects in both of these processes (Bogerd et al., 1994). Strains in which *NUP133* is mutated or partially deleted have been shown to accumulate poly(A)$^+$ RNA in their nuclei after shift to 37°C (Doye et al., 1994; Li et al., 1995). Two different ts alleles of *NSP49/NUP49* have been shown to affect poly(A)$^+$ RNA export and protein import differentially (Doye et al., 1994). Inhibition of protein import was reported for wild-type cells in which *NSP1* expression had been shut off for ≥10 h (Mutvei et al., 1992). Despite these findings, none of the nucleoporins has been shown to be directly involved in translocation of substrate through the NPC.

The known yeast nucleoporins have been identified using several distinct experimental approaches including screening of λgt11 expression libraries with antibodies raised against rat liver nuclear envelopes or yeast nucleoskeleton preparations (Davis and Blobel, 1986; Hurt, 1988; Wente et al., 1992; Loeb et al., 1993; Wente and Blobel, 1994), selection for genes whose products interact with the proteins encoded by mutant alleles of the nucleoporins *NSP1* (Wimmer et al., 1992; Fabre et al., 1994) and *NSP49* (Doye et al., 1994) or *RPA190* (encoding the largest subunit of RNA polymerase I) (Yano et al., 1992), and biochemical isolation (Grandi et al., 1993; Wozniak et al., 1994). None of these approaches selected for nucleoporins with specific transport functions.

Here we describe a novel yeast nucleoporin identified on a functional basis. We cloned *RAT7* (ribonucleic acid trafficking) by complementation of the temperature-sensitive growth defect of a mutant *Saccharomyces cerevisiae* strain isolated in a screen for strains with temperature-dependent defects in poly(A)$^+$ RNA export. The *RAT7* gene is essential and encodes a 1,460–amino acid protein containing 25 XXFG and 3 XFXFG degenerate repeats. 12 of the XXFG repeats are embedded in four nearly perfect tandem 26–amino acid repeats. Antiserum to the repeat domain of Rat7p decorated the nuclear periphery in a punctate pattern characteristic of NPC proteins. Shift of *rat7-1* cells to the nonpermissive temperature of 37°C resulted in rapid (within 15 min) accumulation of poly(A)$^+$ RNA in the nucleus, but did not cause concomitant cytoplasmic accumulation of a reporter protein containing a nuclear localization signal. Thin section EM and indirect immunofluorescence of *rat7-1* cells grown at 23°C revealed NPCs clustered toward one region of the nuclear envelope. Partial dispersal of these clustered NPCs occurred within 1 h of a shift of mutant cells to 37°C, and under these conditions, the mutant Rat7p could no longer be detected. The rapid induction of nuclear accumulation of poly(A)$^+$ RNA when mutant cells were shifted to 37°C along with the lack of a detectable effect on protein import are consistent with a direct role for Rat7p in mRNA export.

Materials and Methods

Yeast Strains, Growth Conditions, and Genetic Methods

Table I lists the yeast strains used in this study. The strains were grown in rich media (1% yeast extract, 2% bactopeptone) with either 2% dextrose (YPD), 2% raffinose (YPR), or 2% galactose (YPG), or in synthetic complete media lacking specific amino acids (Rose et al., 1989). Temperature shifts were performed by brief centrifugation to collect cells and resuspension in prewarmed media. Yeast cells were transformed by electroporation using an electroporator (BioRad Laboratories, Melville, NY) and were allowed to recover in rich media with 1 M sorbitol at 23°C for at least 1 h before plating. General genetic manipulations of yeast cells, including strain crosses, sporulation, and tetrad dissection, were performed according to Rose et al. (1989).

Generation and Screening of Temperature-sensitive Mutants

UV mutagenesis of yeast strains FY86 and FY23 (provided by Dr. F. Win-

Table I. Yeast Strains

Strain	Genotype	Comments
FY23	*MAT*a *ura3-52 trp1Δ63 leu2Δ1*	Wild type; derived from S288C; obtained from Dr. Fred Winston
FY86	*MATα ura3-52 his3Δ200 leu2Δ1*	Wild type; derived from S288C; obtained from Dr. Fred Winston
LGtsα230	*MATα ura3-52 his3Δ200 leu2Δ1 rat7-1^{ts}*	Original *rat7^{ts}* isolate
LGY101	*MATα ura3-52 his3Δ200 leu2Δ1 rat7-1^{ts}*	Segregant from 3rd LGtsα230 × FY23 backcross
LGY103	*MAT*a *ura3-52 trp1Δ63 leu2Δ1 rat7-1^{ts}*	Segregant from 3rd LGtsα230 × FY23 backcross
LGY105	*MAT*a/α *ura3-52/ura3-52 leu2Δ1/leu2Δ1 his3Δ200/his3Δ200*	
LGY106	*MAT*a/α *ura3-52/ura3-52 leu2Δ1/leu2Δ1 his3Δ200/his3Δ200 RAT7::HIS3/RAT7* {pLG4: *URA3 RAT7 CEN*}	Heterozygous diploid *rat7* null strain harboring *RAT7* plasmid pLG4
LGY108	*MAT? ura3-52 his3Δ200 leu2Δ1 RAT7::HIS3* {pLG4:*URA3 RAT7 CEN*}	haploid *rat7* null strain harboring *RAT7* plasmid pLG4
LGY110	*MAT? ura3-52 his3Δ200 leu2Δ1 RAT7::HIS3* {pLG8:*LEU2 RAT7.myc CEN*}	haploid rat7 null strain harboring *RAT7.myc* plasmid pLG8
LDY97	*MATα ura3-52 his3 leu2-3,112 nup1::LEU2* {plasmid bearing *nup1-106^{ts} CEN HIS3*}	Obtained from Dr. Laura Davis (Duke University, Durham, NC)
CHS 5-8 (87-3A)	*MATα his5-131*	Obtained from Cold Spring Harbor Yeast Genetics Course, 1990

ston, Harvard Medical School, Boston, MA) and subsequent isolation of temperature-sensitive (ts) strains were carried out as previously described (Amberg et al., 1992). To screen for strains with temperature-dependent nuclear accumulation of poly(A)$^+$ RNA, ts strains were grown overnight at 23°C in YPD and diluted as pools of five strains such that each strain was represented equally, and total cell density was 2–4 × 10^7 cells/ml. Cultures were grown for an additional 2 h at 23°C and then shifted to 37°C for 2 h before harvesting for the in situ mRNA localization assay. Each member of cell pools exhibiting nuclear accumulation of poly(A)$^+$ RNA was retested individually to identify those strains with potential defects in mRNA export.

In Situ mRNA Localization Assay

Cells shifted to 37°C for specified times were collected by centrifugation in a 37°C room, resuspended in 37°C 0.1 M K_2HPO_4, pH 6.5, 4% formaldehyde, and incubated for 90 min at 23°C with gentle agitation. Fixation was ended by washing cells twice with phosphate buffer (0.1 M K_2HPO_4, pH 6.5) and once with wash buffer (0.1 M K_2HPO_4, pH 6.5, 1.2 M sorbitol) at 23°C. Cells were resuspended in 1 ml wash buffer and stored at 4°C for up to 18 h. Processing of fixed cells was carried out essentially as described previously (Amberg et al., 1992) with a modification of the permeabilization step. All incubations and washes were performed at 23°C unless otherwise noted. Cells in 1 ml of wash buffer were treated with 300 μg 100T Zymolyase (Seikagaku America Inc., Rockville, MD) until 90% of the cells were no longer refractile (appearing grey) as visualized by phase contrast microscopy (15–60 min depending on the strain and length of temperature shift). These spheroplasted cells were washed gently, resuspended in wash buffer, and allowed to adsorb to polylysine-coated wells of teflon-faced slides for 10 min. Adhered cells were incubated successively with phosphate buffer, phosphate buffer with 0.1% NP-40, and phosphate buffer (5 min each), followed by 0.1 M triethanolamine, pH 8.0 for 2 min, triethanolamine with 0.25% acetic anhydride for 10 min, and 4× SSC (1× SSC = 0.15 M NaCl, 0.015 M sodium citrate) for 5 min. Cells were incubated in prehybridization solution (50% formamide, 10% dextran sulfate, 4× SSC, 1× Denhardt's solution, 125 μg of tRNA/ml, 500 μg of denatured sonicated salmon sperm DNA) at 37°C for 1 h in a humid chamber. Oligo dT_{50} was endlabeled with digoxigenin-dUTP using terminal deoxynucleotidyl transferase as described previously (Amberg et al., 1992). Hybridization with prehybridization solution containing 500 pg/ml of digoxigenin-labeled $(dT)_{50}$ probe was carried out for 18 h at 37°C in a humid chamber. Cells were washed for 1 h in 2× SSC, 1 h in 1× SSC, 30 min in 0.5× SSC at 37°C, and 30 min in 0.5× SSC. The cells were equilibrated in antibody wash (ABW) 1 (0.1 M Tris, pH 9.0, 0.15 M NaCl) for 5 min and blocked in ABW1 containing 5% heat-inactivated FCS and 0.3% Triton X-100 for 1 h. The cells were incubated in ABW1 containing 5% FCS, 0.3% Triton X-100, and fluoresceinated antidigoxigenin Fab fragments (Boehringer Mannheim Corp., Indianapolis, IN) for 4 h in the dark. Unbound antibody was removed by washing with ABW1 first for 10 min, then for 30 min, followed by washing with ABW2 (0.1 M Tris, pH 9.5, 0.1 M NaCl, 50 mM $MgCl_2$) first for 10 min, and then for 30 min. The nuclei were counterstained with 4,6-diamidino-2-phenylindole (DAPI) (10 μg/ml in ABW2) for 5 min and then washed twice (5 min each) with ABW2. The slides were mounted under 90% glycerol, 1× PBS containing 1 mg of *p*-phenylenediamine per ml, and stored at −20°C.

Cloning and Sequencing of RAT7

The *RAT7* gene was cloned by complementation of the ts growth phenotype of strain LGY101 with a YCp50-based *S. cerevisiae* genomic library (a generous gift of Dr. Phil Hieter, Johns Hopkins University, Baltimore, MD). A 7.2-kb restriction fragment common to three overlapping, complementing clones was subcloned into pMOB (Gold Biotechnology, St. Louis, MO), and the resulting plasmid was introduced into a bacterial strain (DPWC) harboring TN1000 for random transposon insertion (Gold Biotechnology). With primers complementary to both transposon ends, sequence was generated from both strands by the dideoxy chain termination method (Sanger et al., 1977) using denatured, double-stranded DNA, [α-^{35}S]dATP (New England Nuclear, Boston, MA) and Sequenase version 2.0 (United States Biochemical Corp., Cleveland, OH.). The DNA and predicted protein sequences were compared to the GenBank and EMBL data bases using FASTA and BLAST programs (Altschul et al., 1990; Pearson, 1994). The accession number for this sequence is L40634.

Disruption of RAT7 and Targeted Integration of LEU2 at the RAT7 Locus

To facilitate both construction of a *rat7* null allele and targeted integration of *LEU2* adjacent to the *RAT7* locus, a 7.5 kb EcoRI genomic DNA fragment from complementing clone pLG1 was subcloned into YIplac128 (Gietz and Sugino, 1988) from which polylinker restriction sites between and including HindIII and SmaI had been removed. This yielded pLG5. Disruption of *RAT7* was accomplished by removal of a 4,036-bp HpaI (partial)/NsiI fragment from the 4,380-bp *RAT7* open reading frame (ORF) in pLG5, followed by insertion of a *HIS3*-containing 1,068-bp Eco47III/NsiI fragment from pRS403 (Stratagene, La Jolla, CA). Resulting pLG6 was digested with EcoRI to generate a 4.5-kb linear *RAT7::HIS3* disruption fragment, which

was used to transform diploid yeast strain LGY105. Southern blot analysis of His$^+$ transformants identified heterozygous diploid strains with correct replacement of one allele of *RAT7*. One such strain was transformed with pLG4 (*RAT7* under control of its own promoter on a *URA3*-marked *CEN* plasmid) yielding LGY106, which was sporulated and dissected onto YPD plates. Strains arising from spores were replica plated onto plates lacking histidine and onto plates containing 5-fluoroorotic acid (PCR Inc., Gainesville, FL) and grown at 23°C.

Targeted integration at the *RAT7* locus was performed as described previously (Guthrie and Fink, 1991). *LEU2*-marked pLG5 was linearized at a unique PstI site within the *RAT7* ORF and introduced into a haploid ts *rat7-1* strain. Southern blot analysis of Leu$^+$ transformants was performed to identify strains that had homologously recombined linear DNA into the genomic *RAT7* locus, thereby abrogating temperature sensitivity. Positive strains were crossed with a strain carrying the *rat7-1* allele and sporulated. Spores were tested for growth on YPD plates at 37°C or on plates lacking leucine at 23°C.

Preparation of Rat7p Antiserum

To generate a Rat7p antigen, we constructed a plasmid encoding glutathione S-transferase (GST) fused in frame with amino acids 486–779 of Rat7p. The ends of a ScaI-AvaII fragment from the *RAT7* ORF were blunted using the Klenow fragment of DNA polymerase I, and the fragment was inserted into pGEX-3X (Pharmacia Corp., Piscataway, NJ) that had been linearized with SmaI. *Escherichia coli* DH5α were transformed with the resulting plasmid. Fusion protein was expressed in and purified from bacteria according to published methods (Ausubel et al., 1988). Briefly, a 1-liter culture was grown to an OD_{600} of 0.8 and isopropyl β-D-thiogalactopyranoside (IPTG) was added to induce expression of the fusion protein. Cells were grown an additional 4 h and then lysed by sonication. Fusion protein was purified from the cell extract by chromatography on a glutathione–agarose column (Sigma Chemical Co., St. Louis, MO) and eluted with reduced glutathione (Sigma Chemical Co.). Guinea pigs were inoculated with 50 μg of purified fusion protein and then given 25-μg boosts after 2, 3, 7, and 11 wk. Cocalico Biologicals (Reamstown, PA) performed all immunizations and bleeds.

Epitope Tagging of Rat7p

To prepare myc-tagged Rat7p, a 120-bp DNA fragment encoding three consecutive myc epitopes (EQKLISEEDLN) was released from pKK-1 (obtained from G. Fink, Massachusetts Institute of Technology, Cambridge, MA) by BamHI digestion and inserted into a unique BamHI site (corresponding to amino acid 623) in the *RAT7* ORF. To prepare hemagglutinin (HA)-tagged Rat7p, we synthesized two complementary oligonucleotides, which, when annealed, encode the HA epitope (YPYDVPDYA) and have PstI ends. The oligonucleotides were heated to 90°C, slowly cooled to permit annealing, and inserted into the unique PstI site (corresponding to amino acid 456) in the *RAT7* ORF. Subclones were screened to identify those with the tags in the coding orientation. This yielded pLG8, a *LEU2*-marked *CEN* plasmid encoding myc-tagged RAT7p under the control of its own promoter, and pLG9, a *URA3*-marked *CEN* plasmid encoding HA-tagged RAT7p under the control of its own promoter. pLG8 was electroporated into LGY108, a *RAT7*::*HIS3* null strain carrying a *URA3*-marked *CEN* plasmid containing wild-type *RAT7* (pLG4). Leu$^+$ transformants were grown on plates containing 5-FOA to cure cells of pLG4, yielding LGY110. The only *RAT7* gene in this strain encodes myc-tagged Rat7p. pLG9 was electroporated into wild-type cells, and Ura$^+$ transformants were selected.

Immunofluorescence Procedures

Indirect immunofluorescence was performed as described previously (Copeland and Snyder, 1993). Cells were fixed by adding 0.1 vol of 37% formaldehyde to cell cultures and incubating with gentle agitation for 1 h at 23°C. After three washes with 1.2 M sorbitol, 50 mM K_2HPO_4, pH 7.5 (solution A), cells were resuspended in 1 ml of solution A containing 300 μg 100T Zymolyase (Seikagaku America Inc.) and incubated at 23°C for 10–60 min until spheroplasts were generated. These spheroplasts were washed gently once with solution A and adhered to poly-L-lysine–coated 12-well slides. Cells in these wells were washed sequentially with PBS containing 0.1% BSA (solution B), solution B containing 0.1% NP-40, and solution B, with a 5-min incubation per wash. Cells were incubated with primary antibody in solution B overnight at 4°C and then washed again with solution B, solution B containing 0.1% NP-40, and solution B. Cells were incubated with secondary antibody in solution B for 2 h at 23°C and then washed once each with solution B, solution B containing 0.1% NP-40 and 10 μg of DAPI per ml, solution B containing 0.1% NP-40, and solution B. Cells were mounted as for the mRNA localization assay. Anti-myc epitope antibody 9E10 was kindly provided by Dr. J. Michael Bishop (University of California at San Francisco, San Francisco, CA). mAb RL1 was a generous gift of Dr. Larry Gerace (Scripps Institute, La Jolla, CA). Anti-β-galactosidase antibody was purchased from Sigma Chemical Co. Dr. John Aris (University of Florida, Gainesville, FL) kindly provided anti-Noplp mAb A66. Dr. Maurice Swanson (University of Florida, Gainesville, FL) generously provided anti-Nablp/Npl3p mAb 1E4. Secondary antibodies including FITC-labeled goat anti-mouse IgM, FITC-labeled horse anti-mouse IgG, and FITC-labeled goat anti-guinea pig IgG (H+L) were all obtained from Vector Laboratories, Inc. (Burlingame, CA).

EM

All EM-grade reagents were obtained from Electron Microscopy Sciences (Fort Washington, PA). *S. cerevisiae* cells were prepared for ultrastructural analysis using standard protocols (Byers and Goetsch, 1975; Wright and Rine, 1989). Cells were grown in YPD to early log phase, collected on a filter unit, and washed with 0.1 M cacodylate buffer (pH 6.8). Fixation was done by suspending the cells in 3% glutaraldehyde and 0.1% tannic acid in 0.1 M cacodylate buffer (pH 6.8) at room temperature for 2 h. Cells were then washed twice with 50 mM KP_i (pH 7.5). Spheroplasts were prepared by digestion with Zymolyase 100T. Postfixation in 2% osmium tetroxide was done on ice for 1 h, followed by en bloc staining in 2% uranyl acetate for 1 h at room temperature. After a series of graded ethanol dehydrations, cells were embedded in Spurr's resin (hard recipe) (Spurr, 1969). Thin sections were prepared on an ultramicrotome, stained with uranyl acetate and Reynold's lead citrate, and examined on a microscope at 60 kV (model 100CX; JEOL U.S.A. Inc., Peabody, MA).

Analysis of Protein Synthesis

10 μCi of [^{35}S]methionine (New England Nuclear) and a 100-fold molar excess of cold methionine were added to exponentially growing cultures of yeast cells in SC-met media, which had been incubated continuously at 23°C or shifted to 37°C for 1 h before addition of label. To measure incorporation of radioactivity into TCA-precipitable material, aliquots of each culture were removed after 30, 60, 90, 120, and 240 min of labeling and precipitated with 10% TCA. Precipitates were collected on TCA-presoaked glass filters (GF/A), washed sequentially with 10% TCA and 95% ethanol, and dried. [^{35}S]Methinonine incorporation was measured by scintillation counting.

Results

Rapid Nuclear Accumulation of mRNA in a Strain Bearing the Temperature-sensitive rat7-1 Allele

To identify yeast genes involved in nucleocytoplasmic messenger RNA export, we generated ts strains of *Saccharomyces cerevisiae* and screened them to identify strains that accumulated poly(A)$^+$ RNA in their nuclei following a shift to the restrictive temperature. To visualize the subcellular distribution of mRNA in these cells, in situ hybridization was performed with a digoxigenin-tagged oligo $(dT)_{50}$ probe. The probe anneals to the poly(A) tails of mRNA and pre-mRNA molecules and can be detected with fluorescein-labeled antidigoxigenin antibodies (Amberg et al., 1992). Fig. 1 *A* shows wild-type cells that were grown at the nonpermissive temperature of 37°C for 2 h before fixation and in situ hybridization. The presence of fluorescent signal throughout the cells reflects the efficient export of mRNA from the nucleus to the cytoplasm. Wild-type cells grown at 23°C appeared similar, though overall fluorescence was slightly dimmer (data not shown). To date, we have isolated ~1,200 ts mutant strains and examined them for aberrant mRNA localization after growth at 37°C for 2 h. Genes harboring ts mutations that confer temperature-dependent nu-

clear accumulation of poly(A)$^+$ RNA have been named *RAT* genes.

One of the strains isolated by this assay, LGtsα230, bears the ts *rat7-1* allele, which caused rapid nuclear accumulation of mRNA in cells shifted to 37°C. Even at 23°C, *rat7-1* cells displayed a partial mRNA mislocalization phenotype, with more than half of the cells exhibiting a somewhat brighter fluorescent signal in the nuclear region than in the cytoplasm (Fig. 1 *B*). After a 15-min shift to 37°C, nearly 100% of *rat7-1* cells had nuclei that were dramatically brighter than their cytoplasms (Fig. 1 *C*). While nuclear fluorescence remained bright, the cytoplasmic fluorescence faded within 2 h at 37°C (Fig. 1 *D*), suggesting that little or no new mRNA reached the cytoplasm after the shift to 37°C. Almost complete colocalization of FITC (detecting poly(A)$^+$ RNA; Fig. 1 *D*) and DAPI (detecting DNA; Fig. 1 *E*) staining in cells shifted to 37°C for 2 h demonstrated that mRNA accumulated in the nuclei of mutant cells. This mRNA mislocalization phenotype persisted for at least 6 h at 37°C (data not shown).

To determine whether the mRNA export block was reversible, *rat7-1* cells were shifted to 37°C for 2 h and then returned to 23°C for 60 min before processing for in situ hybridization (Fig. 1 *F*). These cells had discernibly more cytoplasmic signal than cells examined after growth at 37°C for 2 h (compare Fig. 1, *F* and *D*). Their cytoplasmic signal was comparable to, if not brighter than, that seen in *rat7-1* cells grown continuously at 23°C (compare Fig. 1, *F* and *B*). Although their nuclei were still bright, these cells appeared to have resumed exporting mRNA at 23°C. Viability data mirror these findings. Almost immediately after a shift to 37°C, *rat7-1* cells stopped dividing without a specific terminal morphology. When returned to 23°C within 24 h, >80% of the cells were able to resume growth and form colonies.

We compared the growth rates of mutant and wild-type cells at both permissive and restrictive temperatures (Fig. 2). Consistent with the partial mRNA mislocalization phenotype exhibited by *rat7-1* cells grown at 23°C, these cells had a doubling time at 23°C of 160 min, which is ~10–15% longer than the 140-min doubling time of wild-type cells grown at the same temperature. Mutant cells rapidly ceased growth after a shift to 37°C.

It would be expected that interruption of mRNA export would lead to a decline in the rate of protein synthesis. To examine this, cultures of wild-type and *rat7-1* cells that had been grown to early log phase at 23°C were either left at 23°C or shifted to 37°C. After an additional hour of growth, [^{35}S]methionine was added to all cultures and the rate of incorporation into protein examined. Wild-type cells incorporated [^{35}S]methionine into protein at approximately the same rate at both 23°C and after a shift to 37°C. Although cells carrying the *rat7-1* mutation displayed a near wild-type rate of incorporation of [^{35}S]methionine into protein at 23°C, the rate fell to <10% of the wild-type rate within 60 min of a shift to 37°C (data not shown).

Cloning and Sequencing of RAT7

The *RAT7* gene was cloned by complementation of the ts growth phenotype of yeast strain LGY101 using an *S. cerevisiae* genomic library. LGY101 is a segregant from the third backcross of the original *rat7^{ts}* isolate, LGtsα230. Temperature sensitivity and nuclear accumulation of poly(A)$^+$ RNA cosegregated in 24 out of 24 segregants tested from the third backcross, indicating that a single mutant allele confers both phenotypes. Those library plasmids that corrected the temperature-sensitive growth defect of strain LGY101 were tested for their ability to restore mRNA export to *rat7-1* cells grown at 37°C. All clones that could were related, based on restriction endonuclease digestion patterns. Sequencing of a region common to three different complementing clones revealed an open reading frame encoding a protein of 1,460 amino acids (Fig. 3) with a predicted molecular mass of 159 kD. This was consistent with Northern blot analysis, which indicated that the DNA fragments sequenced hybridized to a transcript of 4.4 kb (data not shown). Expected consensus sequences for transcription and translation initiation signals were found in the sequence upstream of the *RAT7* ORF.

Analysis of the primary amino acid sequence revealed that Rat7p contains three different classes of repeats, most of which are clustered in the central third of the protein. As shown in Figs. 3 and 4, there are 25 degenerate XXFG repeats and 3 degenerate XFXFG repeats. 12 of the XXFG repeats are found within four nearly perfect 26–amino acid repeats. Repeats containing the uncommon combination of phenylalanine (F) followed by glycine (G) have been found in a majority of sequenced yeast nucleoporins. Nup49p/Nsp49p, Nup100p, Nup116p/Nsp116p (Wente et al., 1992; Wimmer et al., 1992), and Nup145p (Fabre et al., 1994; Wente and Blobel, 1994) all contain GLFG repeats. Nsp1p (Hurt, 1988), Nup1p (Davis and Fink, 1990), and Nup2p (Loeb et al., 1993) contain multiple XFXFG degenerate repeats that form the cores of 9 amino acid repeats that are loosely related in Nup1p and Nup2p and highly conserved in Nsp1p. Examination of the Rat7p XXFG repeats (Fig. 4) reveals that PSFG and SAFG are found most frequently. There is no clear consensus sequence for the Rat7p XFXFG repeats. 25% of Rat7p amino acids are charged, with 50% more acidic residues than basic resulting in a low isoelectric point of 4.5. The charges are distributed fairly evenly throughout the protein. Secondary structure programs predict that the COOH-terminal third of the protein is largely α helical, unlike the central repeat region, which is rich in proline (P). Furthermore, within the COOH-terminal third is a region (amino acids 1,281–1,301) predicted to have the potential to form coiled-coil interactions (Lupas et al., 1991). The segments from amino acids 1,303–1,316 and 1,392–1,412 have a lower but significant probability of also forming coiled-coil interactions. The NH_2-terminal third has no apparent distinguishing characteristics. Analysis of the protein sequence did not reveal any functional motifs such as RNA binding domains, transmembrane domains, or zinc fingers. There are many potential phosphorylation sites within Rat7p.

A FASTA search of the SwissProt and EMBL data bases for proteins with homology to Rat7p yielded five yeast nucleoporins among the highest scoring sequences. Nup49p/Nsp49p shares 25.8% amino acid identity with Rat7p over a stretch of 151 residues. Nup1p, Nup2p, and Nup100p have 16–19% identity over 380–510 amino acids, and Nsp1p has 21% identity over 408 amino acids. In all five cases, the regions of homology map to the repeat region of Rat7p between amino acids 480 and 980 (see Fig. 5). Two vertebrate nucleoporins, Nup153p and Nup214p, showed ~25% identity with the Rat7p repeat region over 313 and 195 amino

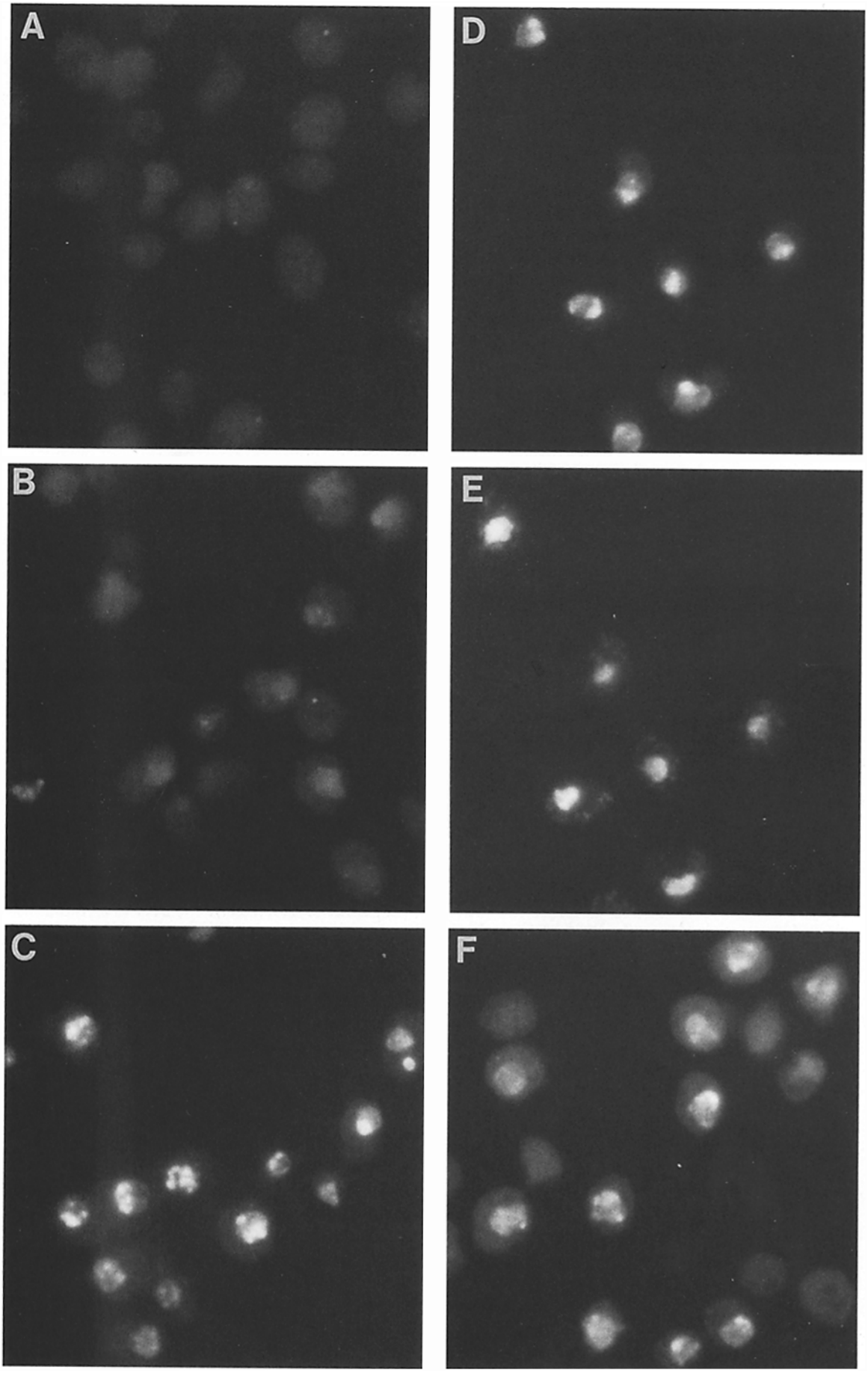
A
D
B
E
C
F

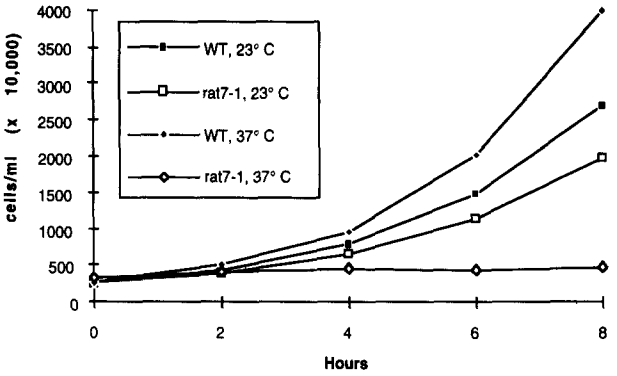

Figure 2. Analysis of growth rates of wild-type and *rat7-1* strains. LGY101 (*rat7-1*) and FY86 (wild type) were grown to stationary phase, diluted back to early log phase, and cultured at either 23°C or 37°C with vigorous aeration. Duplicate culture samples were removed every 2 h, and cells were counted using a hemacytometer. Each data point is the average of cell counts from duplicate samples.

acids, respectively. These homologies strongly suggest that Rat7p is a nucleoporin.

RAT7 is an Essential Gene on Chromosome IX

To determine whether *RAT7* is an essential gene, we performed standard gene replacement and plasmid rescue (Guthrie and Fink, 1991). We removed 4,036 bp out of the 4,380-bp *RAT7* ORF and replaced them with the *HIS3* gene (Fig. 5). Haploid cells bearing the disrupted allele were unable to grow without a plasmid-borne *RAT7* gene, indicating that *RAT7* is essential for mitotic growth of *S. cerevisiae.*

The chromosomal location of *RAT7* was determined by hybridizing labeled *RAT7* DNA to an ordered set of λ clones representing most of the yeast genome (obtained from Riles, L., Washington University, St. Louis, MO, and M. V. Olson, University of Washington, Seattle, WA). The *RAT7* probe recognized λ clone 4210, which maps to the left arm of chromosome IX midway between the centromere and telomere. We confirmed this physical mapping with genetic mapping of the *rat7-1* allele against *his5-131.* The *HIS5* gene has also been mapped to λ clone 4210. Based on the segregation data from the genetic cross (10 parental ditypes, 2 tetratypes, 0 nonparental ditypes), the calculated distance between the two loci is ~10 cM. Agreement between physical and genetic mapping data suggested that the gene we cloned was *RAT7* rather than a suppressor of the *rat7-1* allele. To rule out the possibility that it was a tightly linked suppressor, we performed targeted integration of the *LEU2* gene into the chromosomal locus corresponding to cloned *RAT7* and genetically mapped *LEU2* against *rat7-1.* In 26 out of 27 tetrads analyzed, there was no recombination between the two loci. Thus, the cloned gene maps to the same locus as *rat7-1* and is its wild-type counterpart.

Rat7p Localizes to the Nuclear Pore

To immunolocalize Rat7p, polyclonal antiserum was raised in guinea pigs against a GST-Rat7 fusion protein containing amino acids 486–779 of Rat7p. This portion of Rat7p contains 19 of the 25 XXFG repeats, 2 of the 3 XFXFG repeats, and all 4 of the 26-amino acid repeats (Fig. 3). By Western blot analysis, the antiserum identified a single band in an extract of total protein from wild-type cells (Fig. 6, lane *7*). Under various gel conditions, the detected protein migrated with an apparent molecular mass of 205 kD.

Because the protein detected by Western blot analysis migrates during electrophoresis as if it were ~46 kD greater than the 159 kD predicted for Rat7p from the DNA sequence, we investigated whether the protein recognized by the GST-Rat7p antiserum was indeed Rat7p rather than a larger protein antigenically related to it. For this purpose, Rat7p was epitope tagged in two ways, either by inserting DNA encoding three tandem "myc" epitopes into *RAT7* at the unique BamHI site corresponding to amino acid 623, or by inserting DNA encoding a single HA epitope into the unique PstI site corresponding to amino acid 456 (Fig. 5). The plasmid encoding $Rat7p_{myc}$ was introduced into a *RAT7::HIS3* null strain by standard plasmid shuffle procedures (Guthrie and Fink, 1991). This tagged version of Rat7p provided essential Rat7p function(s) insofar as it rendered the null strain viable, albeit slower growing than wild type at 23°C (data not shown). The plasmid encoding $Rat7p_{HA}$ was introduced into wild-type cells. Using extracts from the strains bearing the epitope-tagged alleles, we tested whether the proteins immunoprecipitated by anti-myc mAb 9E10 (Evan et al., 1985) and anti-HA mAb 12CA5 (Berkeley Antibody Co., Richmond, CA) were recognized by the anti-GST-Rat7p serum on a Western blot. For each epitope-tagged strain, protein was detected when the appropriate mAb was used in the immunoprecipitation step and was not detected when the antibodies were switched (Fig. 6, lanes *1–4*). Immunoprecipitation of $Rat7p_{HA}$ with mAb 12CA5 yielded a barely detectable protein band (lane *3*). Immunoprecipitated $Rat7p_{myc}$ was much more easily detected and, as expected for a protein with 75 additional amino acids, migrated slightly more slowly than wild-type Rat7p (Fig. 6, compare lanes *2* and *7*). The faster migrating bands in lane *2* are presumed to be proteolytic breakdown products. These results demonstrate that the anti-GST-Rat7p serum specifically recognized the Rat7 protein. It is well established that a subset of vertebrate nucleoporins have multiple O-linked *N*-acetylglucosamine residues (Snow et al., 1987). Such glycosylation could account at least par-

Figure 1. Temperature shift of *rat7-1* cells to 37°C rapidly induces a reversible block in mRNA export. Wild-type and *rat7-1* cells were grown to mid-log phase in rich media at 23°C and then subjected to various temperature conditions before fixation and in situ hybridization with a digoxigenin-tagged oligo $(dT)_{50}$ probe for localization of poly(A)$^+$ RNA. *A–D* and *F* show fluorescence signal from representative fields of cells that were probed with FITC-conjugated anti-digoxigenin antibody after hybridization. *E* shows DAPI staining for the same field of cells as in *D.* (*A*) Wild type, 2 h at 37°C; (*B*) *rat7-1*, 23°C; (*C*) *rat7-1*, 15 min at 37°C; (*D* and *E*) *rat7-1*, 2 h at 37°C; (*F*) *rat7-1*, 2 h at 37°C followed by 1 h at 23°C. Identical photographic and printing conditions were used for *A–D* and *F.* Shorter exposure times were used for the single DAPI-stained image (*E*).

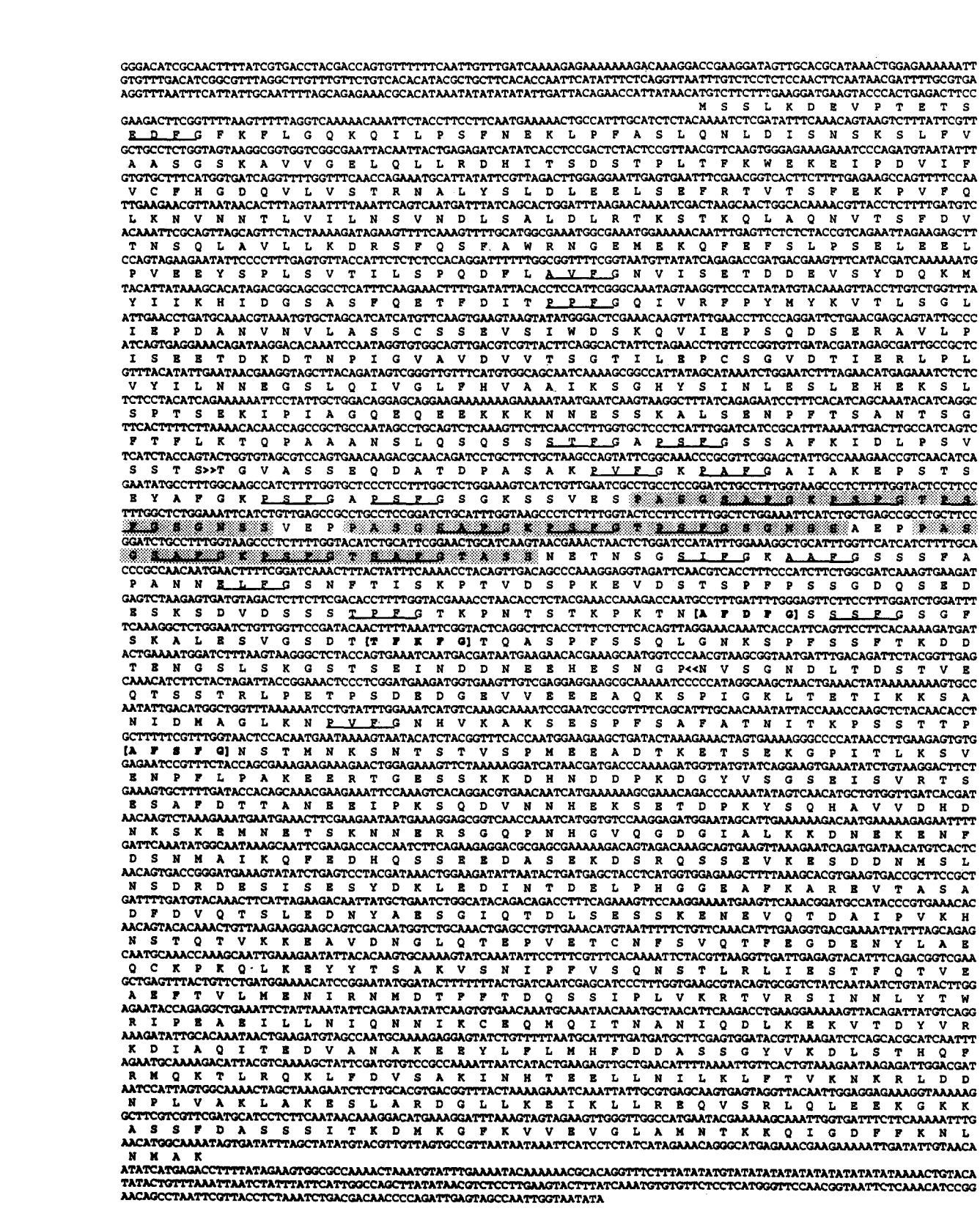

Figure 3. Nucleotide sequence of *RAT7* and predicted protein sequence of Rat7p. 5,094 nucleotides including the 4,380-nucleotide *RAT7* open reading frame are presented. The predicted Rat7p amino acid sequence is shown in single-letter code, and the last amino acid in each line is numbered. XXFG repeats are underlined. XFXFG repeats are bracketed and in bold. Direct repeats of 26 amino acids are shaded gray. The amino acids included in the GST-Rat7 fusion protein are bracketed by >> and <<. These sequence data are available from EMBL/GenBank/DDBJ under accession number L40634.

A

```
14    EDFG  ...
228   AVFG  ...
267   PPFG  ...
462   STFG  A
467   PSFG  SSAFKIDLPSVSSTST
            GVASSEQDATDPASAK
503   PVFG  K
508   PAFG  AIAKEPSTSE
522   YAFG  K
527   PSFG  A
532   PSFG  SGKSSVESPASG
548   SAFG  K
553   PSFG  T
558   PSFG  SGNSSVEPPASG
574   SAFG  K
579   PSFG  T
584   PSFG  SGNSSAEPPASG
600   SAFG  K
605   PSFG  T
610   SAFG  TASSNETNSG
624   SIFG  K
629   AAFG  SSSFAPANN
642   ELFG  SNFTISKPTVDSPKEVDSTSP
            FPSSGDQSEDESKSDVDSSS
687   TPFG  TKPNTSTKPKTNAFDFGS
709   SSFG  ...
842   PVFG
```

B

```
703   KTN  AFDFG  SSSFGSGFSKALESVG
727   SDT  TFKFG  TQASPFSSQLGNKSP...
872   TTP  AFSFG  NST
```

C

```
518   STSEYAFGKPSFGAPSFGSGKSSVES
544   PASGSAFGKPSFGTPSFGSGNSSVEP
570   PASGSAFGKPSFGTPSFGSGNSSAEP
596   PASGSAFGKPSFGTSAFGTA_SSNET
```

Figure 4. Repeats present in Rat7p. (*A*) XXFG degenerate repeats; (*B*) XFXFG degenerate repeats; (*C*) 26-amino acid direct repeats aligned to show homologies. Perfectly conserved amino acids are in bold. Three dots indicate more than 41 amino acids between repeats. Numbers indicate the position of the first amino acid in each repeat.

tially for the discrepancy between the predicted and apparent molecular weight of Rat7p. Thus far, glycosylation of yeast nucleoporins has not been reported. Further investigation will be required to determine the nature of any Rat7p post-translational modifications.

We performed indirect immunofluorescence with the anti-GST-Rat7p serum to localize Rat7p in wild-type cells. As can be seen in Fig. 7 *A*, the antiserum specifically decorated the periphery of the nuclei in a punctate pattern. The DAPI staining region of the same cells (Fig. 7 *B*) was circumscribed by the punctate ring. The same pattern was observed for immunolocalization of $Rat7p_{myc}$ with 9E10 antibodies, but the signal was much weaker (data not shown). Nucleoporins have a stereotypical localization pattern resulting in punctate staining around the periphery of the nucleus as visualized by indirect immunofluorescence. Together, the Rat7p immunolocalization result and the sequence data showing nucleoporin-like repeats in Rat7p indicate that Rat7p is a nucleoporin. Therefore, we refer to this protein as Rat7p/Nup159p.

Analysis of the Distribution of a Karyophilic Reporter Protein in rat7-1 Cells Shifted to the Restrictive Temperature

The NPC supports bidirectional transport of macromolecules across the nuclear envelope. The mutation in the *rat7-1*

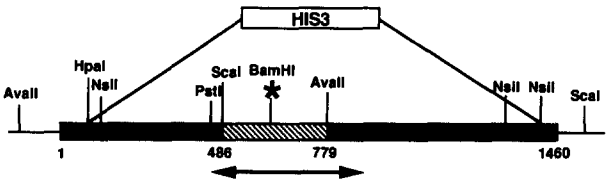

Figure 5. Schematic representation of the *RAT7* locus and modifications made to it. The 4,380-bp *RAT7* ORF is indicated by the long shaded box. DNA flanking the ORF is represented by thin horizontal lines. Within the ORF, a striped section indicates the region used for the GST-RAT7 fusion. For the gene disruption, DNA in between the diagonal lines was replaced with the *HIS3* gene as shown. An asterisk marks the BamH1 site into which DNA encoding three tandem "myc" epitopes was inserted. All restriction sites used in this work are shown. Numbers below the ORF indicate the positions of amino acids corresponding to the sequence junctions shown. The repeat region, which contains all of the repeats except for three NH_2-terminal XXFG repeats, is marked with a double headed arrow.

allele could alter NPC structure in a way that affects all nucleocytoplasmic transport. If this were the case, we would expect that defects in protein import in *rat7-1* cells would occur with kinetics similar to those observed for defects in mRNA export. Alternatively, the *rat7-1* mutation could specifically affect RNA export functions of the NPC.

To determine whether *rat7-1* cells have rapidly induced protein import defects, we analyzed the distribution of a karyophilic reporter protein in *rat7-1* cells. Indirect immunofluorescence was performed to monitor the distribution of a fusion protein containing *E. coli* β-galactosidase and the first 33 amino acids of yeast histone H2B (containing its nuclear localization signal) (Moreland et al., 1987). As a positive control for defects in nuclear protein import, we used strain LDY97, which carries the ts *nup1-106* allele. This

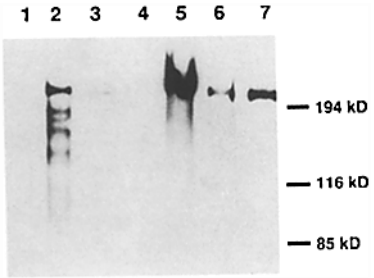

Figure 6. Antiserum raised against GST-Rat7 fusion protein is specific for Rat7p. Extracts were prepared from wild-type cells, wild-type cells transformed with a plasmid encoding HA-tagged Rat7p, and from a *RAT7::HIS3* null strain carrying a plasmid encoding myc-tagged Rat7p. Western blot analysis with GST-Rat7p antiserum was performed on extracts directly (lanes *5–7*) or on protein immunoprecipitated from extracts with α-myc mAb 9E10 or α-HA mAb 12CA5 (lanes *1–4*). (Lane *1*) myc-tagged Rat7p immunoprecipitated with α-HA 12CA5. (Lane *2*) myc-tagged Rat7p immunoprecipitated with α-myc 9E10. (Lane *3*) HA-tagged Rat7p immunoprecipitated with α-HA 12CA5. (Lane *4*) HA-tagged Rat7p immunoprecipitated with α-myc 9E10. (Lane *5*) myc-tagged Rat7p extract. (Lane *6*) HA-tagged Rat7p extract. (Lane *7*) Wild-type extract. Samples were run on a 5% SDS-polyacrylamide gel.

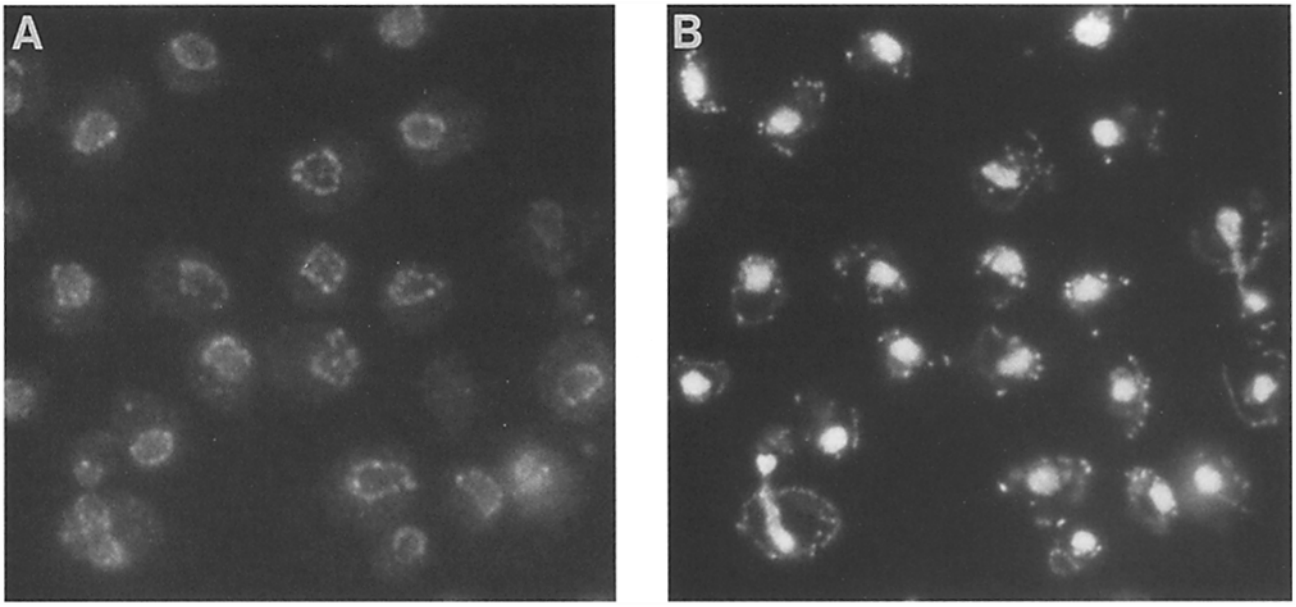

Figure 7. Immunolocalization of the Rat7 protein. Indirect IF was performed on wild-type cells using antiserum raised against a GST-Rat7 fusion protein bearing 292 amino acids from the repeat region (see Figs. 2 and 4) in the central third of Rat7p. *A* shows the fluorescent Rat7p staining pattern. *B* shows the same field of cells stained with DAPI.

strain has been shown to have temperature-dependent defects in both mRNA export and protein import (Bogerd et al., 1994). Wild-type *rat7-1* and *nup1-106* cells were transformed with a plasmid encoding the reporter protein under the control of *GAL10* promoter elements, facilitating high levels of expression upon induction with galactose and repression when glucose is present. However, *nup1-106* cells require >2 h at the nonpermissive temperature to develop an RNA export block, and never show poly(A)$^+$ RNA accumulation in more than a minority of the cells. Therefore, if handled identically to *rat7-1* cells, the *nup1-106* cells would continue to export reporter protein mRNA after the temperature shift, while *rat7-1* cells would cease mRNA export rapidly. To control for this difference, we limited reporter gene transcription to 90 min in all cell types by adding glucose at the end of the induction period.

All three transformed strains were grown to early log phase at 23°C in YPR, rich media containing 2% raffinose (a noninducing carbon source). For unshifted samples, cells were pelleted and resuspended in YPG (2% galactose) to induce reporter gene transcription. After 1.5 h of induction, cells were transferred to YPD (2% dextrose) and grown for 1.5 h more at 23°C before fixation. In both wild-type (Fig. 8 *A*) and *rat7-1* cells (Fig. 8 *B*), reporter protein was detected exclusively in the nucleus, based on colocalization of FITC (Fig. 8) and DAPI staining (data not shown). By contrast, in *nup1-106* cells, reporter protein accumulated in the nucleus but was also clearly detected in the cytoplasm (Fig. 8 *C*), suggesting a partial protein import block in these mutant cells cultured at 23°C. Since *rat7-1* cells show moderate accumulation of mRNA in their nuclei when grown at 23°C (see Fig. 1 *B*), the lack of detectable cytoplasmic accumulation of the reporter protein provides evidence that the moderate defect in mRNA export in *rat7-1* cells does not reflect an overall impairment of nucleocytoplasmic trafficking.

To examine protein import under nonpermissive conditions, *nup1-106* cells were shifted to 36°C for 2 h before galactose induction because it has been shown that these cells require 3 h to show a protein import block (Bogerd et al., 1994). After 2 h of incubation at 36°C, we induced reporter gene expression for 1.5 h at the same temperature. After this induction period, cells were incubated in YPD an additional 1.5 h at 36°C before processing for indirect immunofluorescence. (36°C was used as the non-permissive temperature because we have found that the *GAL10* promoter does not function efficiently at 37°C. We have performed the in situ mRNA localization assay on *rat7-1* cells shifted to 36°C and saw no difference from mutant cells shifted to 37°C; data not shown.) *nup1-106* cells shifted to 36°C showed significantly stronger staining for the reporter protein in their cytoplasms than when grown continuously at 23°C (compare Fig. 8, *F* and *C*). In some cells, the cytoplasm was so bright that a distinct nuclear signal could no longer be discerned.

In *rat7-1* cells, it was necessary to induce the reporter gene at the permissive temperature since the very rapid block to mRNA export at 36°C precluded the production of detectable quantities of reporter protein when induction was performed at 36°C (data not shown). Cultures of wild-type and *rat7-1* cells that had been induced at 23°C for 1.5 h were transferred to 36°C YPD for an additional 1.5 h before fixation. There was no obvious temperature-dependent cytoplasmic accumulation of the reporter protein in either wild-type or *rat7-1* cells (Fig. 8, *D* and *E*). This absence of detectable cytoplasmic reporter protein in *rat7-1* cells shifted to 36°C is compatible with the possibility that rapid development of the mRNA export block in *rat7-1* cells at 36°C is not a consequence of a nonspecific structural collapse of the NPC. This conclusion is supported by the absence of cytoplasmic accumulation of two endogenous nuclear proteins, Noplp and Npl3p, either in cells maintained at 23°C or after a 1-h shift to 37°C (data not shown). However, due to the very rapid

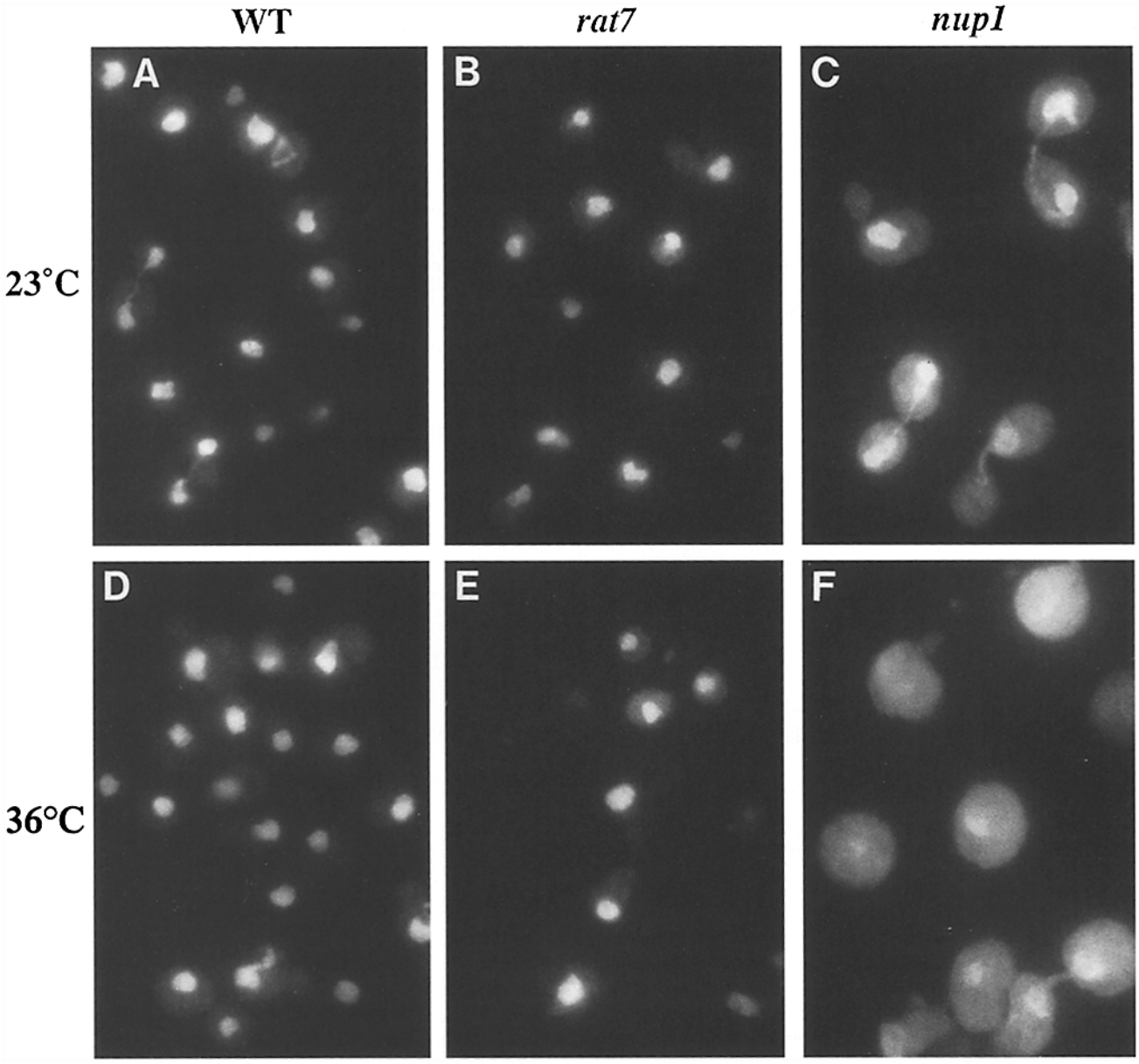

Figure 8. Nuclear import of an overexpressed karyophilic reporter protein in wild-type, *rat7-1*, and *nup1-106* cells. Reporter protein consisting of the histone 2B nuclear localization signal fused to β-galactosidase was overexpressed in three different strains and immunolocalized with anti-β-galactosidase antibody after growth at 23°C or 36°C. All strains were grown to mid-log phase in medium containing raffinose, a noninducing carbon source. Cells shown in *F* were preshifted to 36°C in the same medium. Overexpression of the *GAL10* promoter-driven reporter gene was induced by growth on galactose-containing medium for 1.5 h at 23°C (*A–D*) or 36°C (*F*). After induction, cells were transferred to glucose-containing medium and grown at 23°C (*A–C*) or 36°C (*D–F*) for 1.5 h before processing for indirect IF. (*A* and *D*) Wild type; (*B* and *E*) *rat7-1*; (*C* and *F*) *nup1-106.*

cessation of mRNA export in *rat7-1* cells shifted to 36°C, we cannot be certain that the amount of reporter protein synthesized after the shift to 36°C was sufficient to detect cytoplasmic accumulation. Clearly, *rat7-1* cells do not have a defect in retention of nuclear proteins at the nonpermissive temperature, but additional studies will be required to evaluate the ability of *rat7-1* cells to transport karyophilic proteins to the nucleus.

rat7-1 Mutants Have Aberrant Distribution of NPCs

To determine whether the mutation(s) in the *rat7-1* allele produced any structural and/or localization defects associated with NPCs, immunofluorescence (IF) and EM studies were carried out with mutant cells cultured either at 23°C or shifted to the nonpermissive temperature of 37°C. For IF studies, we used the RL-1 antibody (Snow et al., 1987), which recognizes both mammalian and *S. cerevisiae* NPC proteins (Copeland and Snyder, 1993). Wild-type cells that were grown at either 23°C or shifted to 37°C and stained with RL-1 exhibited punctate staining of moderate intensity all around the nuclear perimeter (Fig. 9 *A*). In contrast, *rat7-1* cells grown at 23°C and stained with RL-1 showed a very strong, continuous signal that was localized to one region of the nuclear periphery (Fig. 9 *B*). Punctate staining

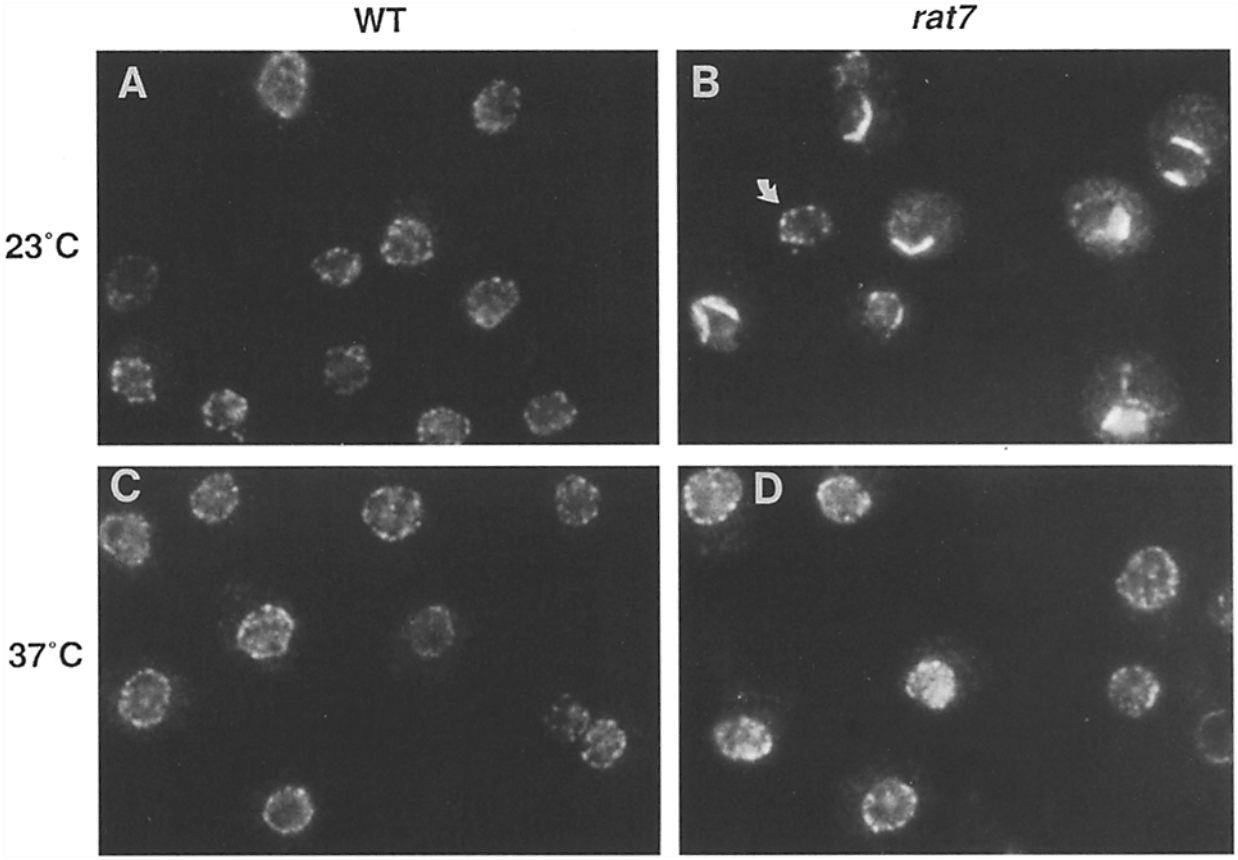

Figure 9. Indirect IF of NPCs in wild-type and *rat7-1* cells. Wild-type and *rat7-1* cells were grown continuously at 23°C or shifted to 37°C for 1 h before fixation and processing for indirect IF. Cells were stained with monoclonal antibody RL-1 (Snow et al., 1987), which recognizes NPC epitopes from various species including rat and *S. cerevisiae*. The fluorescent staining patterns in each of the four panels reflect the intracellular distribution of NPCs. (*A*) Wild type, 23°C; (*B*) *rat7-1*, 23°C; (*C*) wild type, shifted to 37°C for 1 h; (*D*) *rat7-1* shifted to 37°C for 1 h.

around the remainder of the nuclear rim was greatly reduced in intensity, relative to wild-type cells, or was altogether absent. The intensification and melding of signal around part of the nuclear periphery together with the reduction of signal elsewhere suggested that the epitopes detected by RL-1 were clustered together in one region of the nuclear envelope. The degree of "clustering" varied from cell to cell, with staining extending between one quarter and two thirds of the way around the nuclear periphery in a majority of cells. A low percentage of cells displayed immunofluorescence in a single small spot, while even fewer retained an almost wild-type appearance (see cell marked with arrow in Fig. 9 *B*). In all cases, the observed signal was found adjacent to the DAPI-stained region, indicating that the RL-1 antibody staining was at the nuclear periphery (data not shown). Using Rat7p antiserum together with RL-1, we performed double staining of *rat7-1* cells grown at 23°C and found that the staining patterns for each antibody were coincident (data not shown).

Surprisingly, *rat7-1* cells that were shifted to 37°C for 1 h displayed RL-1–reactive antigens distributed around the nuclear periphery in a pattern more similar to that of wild-type cells (Fig. 9 *D*) than that of mutant cells at 23°C. Fewer than 20% of the cells examined exhibited residual clustering. To determine whether this change in NPC distribution seen when *rat7-1* cells were shifted to 37°C could be correlated with alterations in the association of Rat7p with NPCs, we performed indirect IF using the anti-Rat7p antibodies described above. In cells cultured at 23°C, Rat7p was detected at the nuclear periphery in both wild-type (Fig. 10 *A*) and *rat7-1* cells (Fig. 10 *B*). As expected, NPCs appeared clustered in mutant cells. When mutant cells that had been shifted to 37°C for 1 h were stained with these antibodies, >95% of the cells showed no staining for Rat7p at the nuclear periphery (Fig. 10 *E*). In contrast, wild-type cells showed a normal punctate nuclear rim staining pattern under these conditions (Fig. 10 *D*). When these cells were stained with the RL1 antinucleoporin antibody, the same pattern was seen as is shown in Fig. 9 *D* (data not shown).

To further substantiate the observations made via indirect IF, wild-type and *rat7-1* mutant cells were prepared for viewing by thin section EM. Cells were grown continuously at 23°C or shifted to 37°C for 1 h before fixation. Examination of wild-type cells exposed to both temperatures showed that the NPCs were more or less evenly distributed around the nuclear envelope (Fig. 11, *A* and *C*). In agreement with the IF studies, *rat7-1* cells grown at 23°C had many but not all NPCs clustered together within the plane of the nuclear envelope (Fig. 11 *B*). This clustering dispersed to some extent upon shifting the cells to 37°C (Fig. 11 *D*), as also noted by indirect IF. Whereas many *rat7-1* cells grown at 23°C had clusters of 6–10 NPCs, relatively few *rat7-1* cells shifted to 37°C had clusters of >4 NPCs. Other than the clustering of

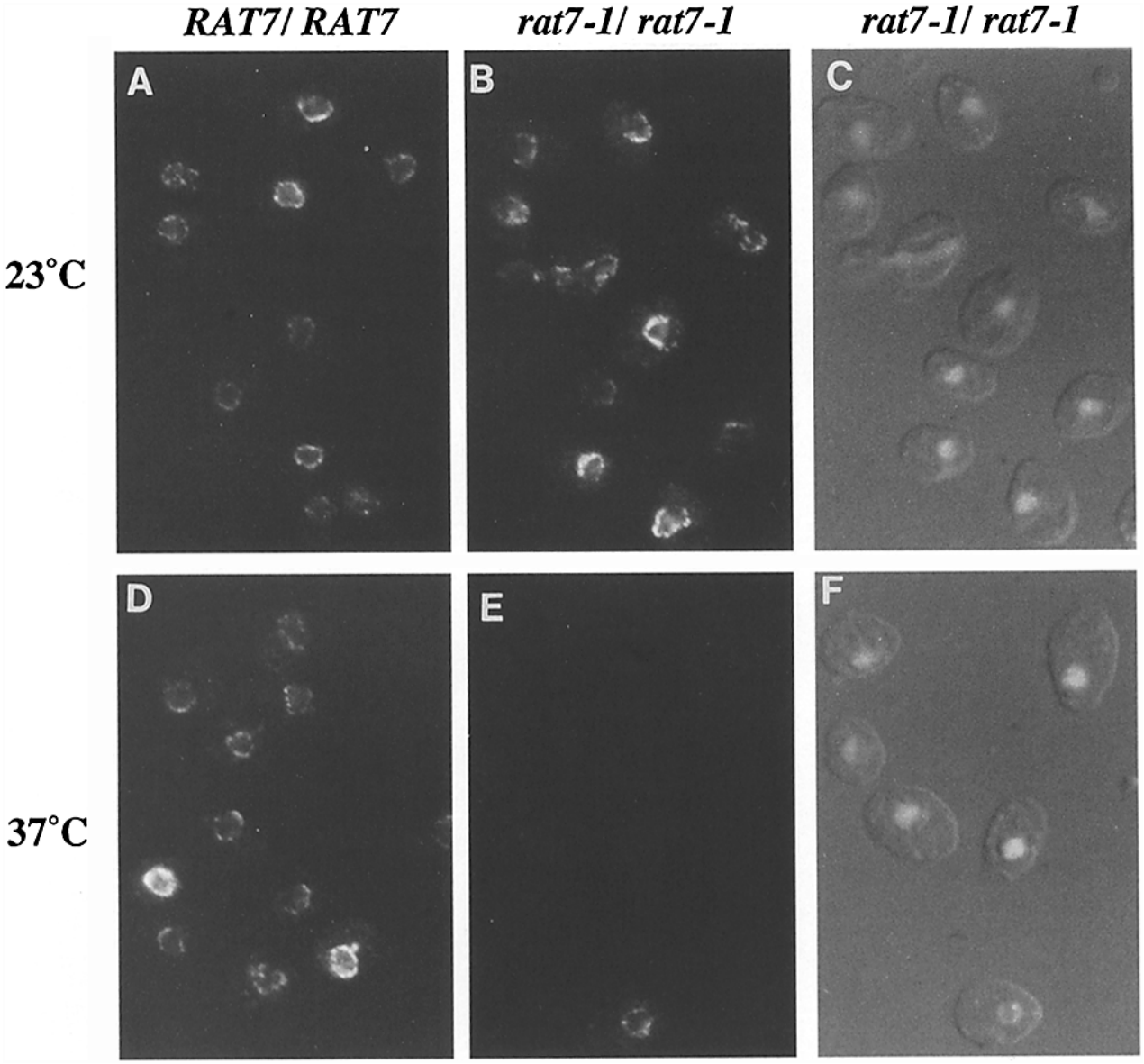

Figure 10. Indirect IF to determine whether mutant Rat7p/Nup159p is present in NPCs of *rat7-1* cells. Wild-type and mutant *rat7-1* cells were grown to early log phase and either maintained at 23°C or shifted to 37°C for 1 h before fixation and processing for indirect IF. Cells were stained with anti-Rat7p antibodies reactive with the repeat domain of Rat7p/Nup159p and with FITC-conjugated goat anti-guinea IgG. (*A*) Wild type, 23°C, FITC; (*B*) *rat7-1*, 23°C, FITC; (*C*) the same field of cells as in *B* stained with DAPI; (*D*) wild type, shifted to 37°C for 1 h, FITC; (*E*) *rat7-1*, shifted to 37°C for 1 h, FITC; (*F*) the same field of cells as in *E* stained with DAPI.

pores in the plane of the nuclear envelope, no significant abnormalities were observed with the NPCs or nuclear envelope in *rat7-1* cells.

We also investigated whether any of the phenotypes associated with the *rat7-1* mutation were dominant by examining growth, poly(A)$^+$ RNA localization, and NPC distribution in strains heterozygous either for the *rat7-1* mutation or for disruption of the *RAT7* gene. These properties were examined at both 23°C and 37°C. We found that both types of heterozygotes were fully wild type for all three phenotypes. At both temperatures, they grew at wild-type rates and to the same density as wild-type diploids; they exhibited no mRNA export defect; and they displayed a wild-type NPC distribution pattern (data not shown). Thus, the *rat7-1* mutation is fully recessive.

Discussion

We have identified a novel *S. cerevisiae* nucleoporin, Rat7p/Nup159p, on the basis of its involvement in mRNA export. We cloned the *RAT7/NUP159* gene by complementation of the ts growth defect of a mutant yeast strain that accumulated poly(A)$^+$ RNA in its nuclei within 15 min of a shift to the restrictive temperature. 2 h after the shift, nuclear poly(A)$^+$ RNA concentration remained elevated, but cytoplasmic poly(A)$^+$ RNA was no longer detectable, indicating that export of newly synthesized mRNA had been blocked. The gene is essential for yeast viability and is predicted to encode a 1,460–amino acid protein with a molecular mass of 159 kD.

Several lines of evidence show that Rat7p/Nup159p is a

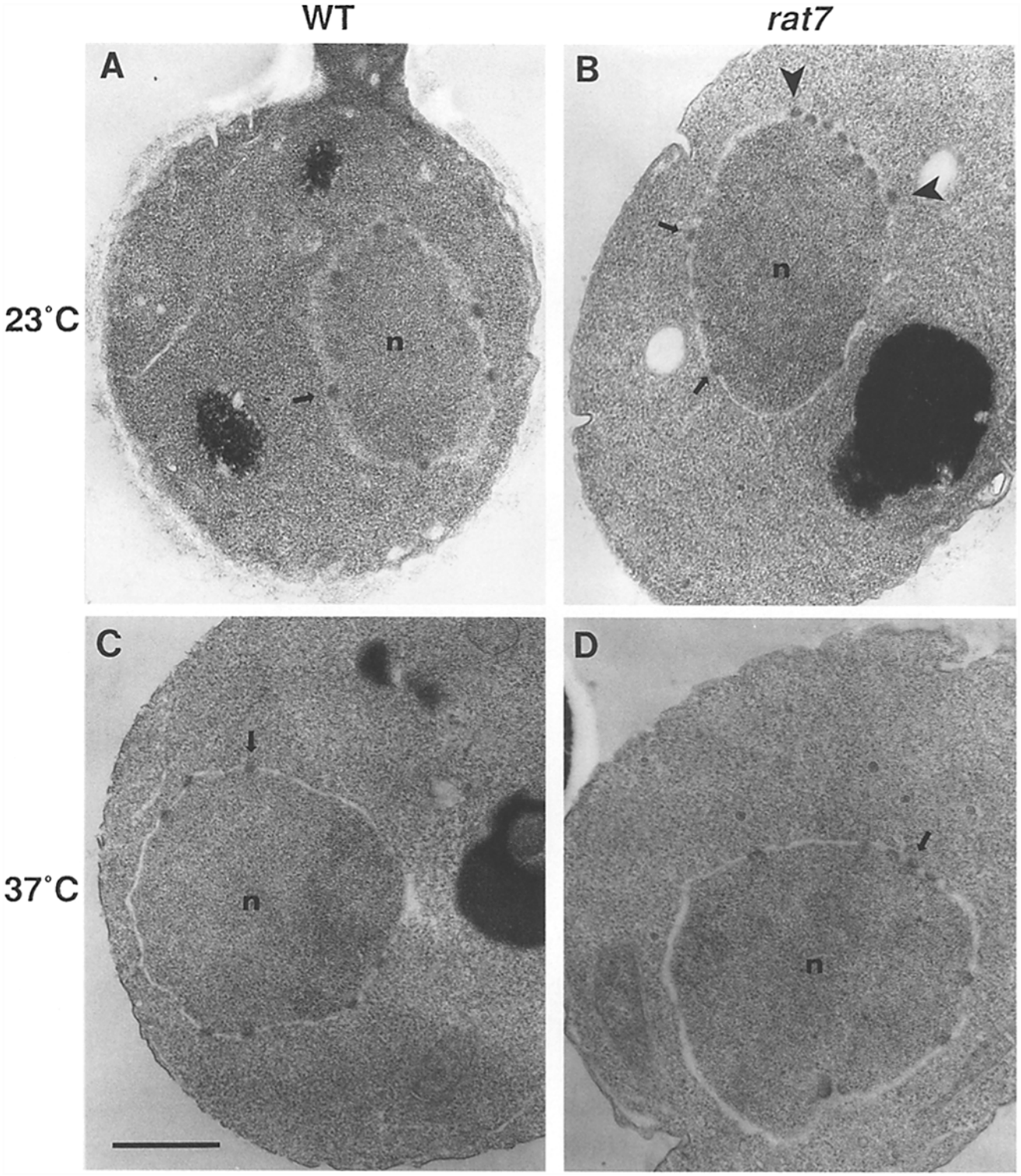

Figure 11. Electron micrographs of the nuclear region of wild-type and *rat7-1* cells grown at 23°C or shifted to 37°C for 1 h. Cells were grown to early log phase and prepared for ultrastructural analysis as described in Materials and Methods. (*A*) Wild type, 23°C; (*B*) *rat7-1*, 23°C; (*C*) wild type, shifted to 37°C for 1 h; (*D*) *rat7-1*, shifted to 37°C for 1 h. Arrows denote representative NPCs in each cell. Large arrowheads denote a cluster of NPCs in a *rat7-1* cell grown at 23°C. *n*, nucleus. Bar, 1 μm.

nucleoporin. First, as seen by indirect IF, antibody specific for Rat7p/Nup159p stained the nuclear periphery in a punctate pattern diagnostic of NPCs. Second, the Rat7p/Nup159p amino acid sequence contains multiple tetrapeptide and pentapeptide repeats closely related to repeats previously found in many yeast and several mammalian nucleoporin sequences. The only proteins in the data base at present that contain these repeats are NPC proteins. Several yeast and

vertebrate nucleoporins share significant amino acid homology with Rat7p/Nup159p within its repeat region. Third, by both IF and EM analyses, cells bearing the ts *rat7-1* allele exhibited aberrant NPC distribution with the majority of NPCs clustered toward one side of the nucleus. NPC clustering has been reported for yeast strains bearing partial deletions of nucleoporins *NUP145* and *NUP133* (Doye et al., 1994; Wente and Blobel, 1994). Finally, the *rat7-1* allele is synthetically lethal with a ts-sensitive allele of *RAT3* (Gorsch, L. C., and C. N. Cole, unpublished results), which is identical to the nucleoporin *NUP133* (Doye et al., 1994; Li et al., 1995).

Repeat Motifs of Rat7p/Nup159p

Many of the yeast nucleoporins sequenced to date have been assigned to subfamilies based on the presence of highly repeated GLFG or XFXFG motifs in their protein sequences. These repeats have been defined not only by their sequences but also by the amino acids that separate them. GLFG repeats are generally separated by spacer sequences of five or more amino acids rich in asparagine, glutamine, serine, and threonine. Rat7p/Nup159p contains 25 XXFG degenerate repeats that differ from GLFG repeats both in their primary sequences and in their spacer sequences. As shown in Fig. 4 *A*, the majority of the tetrapeptide repeats are either PSFG or SAFG. Though replete with serines, the spacer sequences are not unusually rich in asparagine, glutamine, or threonine and often consist of only a single amino acid. Rat7p/Nup159p also contains three XFXFG degenerate repeats that differ from those in other nucleoporins in that they are far less abundant, do not form the cores of longer repeats, and do not have highly charged spacer sequences (Fig. 4 *B*).

Various monoclonal antibodies raised against rat liver nuclear envelopes have been shown to recognize multiple members of either the GLFG or XFXFG nucleoporin subfamilies (Aris and Blobel, 1989; Davis and Fink, 1990; Wente et al., 1992). Presumably, these antibodies bind an epitope common to the repeat regions of these proteins. By contrast, polyclonal antiserum raised against a GST-Rat7/Nup159 fusion protein bearing 19 XXFG repeats and 2 XFXFG repeats detected only a single band on a Western blot of total yeast protein. The repeat region of Rat7p/Nup159p appears to be antigenically unique, suggesting that the repeats in Rat7p/Nup159p are not present in other yeast nucleoporins. 12 of the 19 XXFG repeats included in the fusion protein are embedded in 4 nearly perfect 26-amino acid repeats (see Fig. 3). Such highly conserved, extended repeats have not been found in other yeast or metazoan nucleoporins and may impose a higher order structure on the shorter repeats.

NPC Clustering

We have shown by IF and thin section EM that *rat7-1* cells grown at 23°C have an aberrant distribution of NPCs. Instead of being evenly spaced around the nuclear envelope as in wild-type cells, the majority of NPCs in mutant cells are clustered together in one region of the nuclear periphery. More than 50% of *rat7-1* cells grown at 23°C exhibited some nuclear accumulation of poly(A)$^+$ RNA, perhaps as a consequence of reduced mRNA export through clustered NPCs. Transfer of *rat7-1* cells to 37°C for 1 h exacerbated this mRNA export defect dramatically while, paradoxically, restoring near wild-type distribution of NPCs. Thus, NPC clustering by itself can occur (as in *rat7-1* cells at 23°C) without causing a powerful block to mRNA export or dramatic reductions in growth rate; conversely, a wild-type or nearly wild-type distribution of NPCs (as in *rat7-1* cells at 37°C) does not ensure that other NPC functions, in this case mRNA export, occur normally. The finding that Rat7p could not be detected in NPCs after a shift of mutant cells to 37°C (Fig. 10) suggests that loss of Rat7p from mutant NPCs permitted them to regain a more normal distribution within the nuclear envelope but dramatically decreased their ability to export poly(A)$^+$ RNA.

Mutations in five nucleoporin genes identified to date result in altered NPC distribution and/or nuclear envelope morphology. These phenotypes—nuclear envelope herniation, nuclear envelope projections, and nuclear pore clustering—seem to reflect three separable defects. (*a*) In *nup145ΔN* cells, which lack most of the amino half of *NUP145*, NPCs are found in "grapelike" clusters where they aggregate into amorphous masses (Wente and Blobel, 1994). Within these clusters, NPCs underlie successive herniations in the nuclear envelope. In *nup116Δ* cells shifted to 37°C, NPCs are distributed in a wild-type pattern but have membranous seals overlying their cytoplasmic faces (Wente and Blobel, 1993). The nuclear envelope herniations associated with NPCs in these mutants have been suggested to reflect a defect in the attachment of the NPC to the surrounding pore membrane and a weakening of the boundary that normally separates the two (Wente and Blobel, 1994). (*b*) Various *nupl* mutants have misshapen nuclei with projections of the nuclear envelope extending from the body of the nucleus into the cytoplasm. Within these deformed nuclear envelopes, NPCs have essentially wild-type morphology and spacing (Bogerd et al., 1994). These nuclear envelope projections have been taken to indicate a dissociation of the NPCs from underlying nucleoskeletal elements (Bogerd et al., 1994). (*c*) Both deletion and mutation of *NUP133* result in NPC clusters that are not associated with gross perturbations of the nuclear envelope (Doye et al., 1994; Li et al., 1995). Likewise, in *rat7-1* cells grown at 23°C, NPCs are indistinguishable from those in wild-type cells except for their spacing. They remain aligned in the plane of the nuclear envelope, which itself appears normal. Thus, although NPC clustering and nuclear envelope deformation were both seen in *nup145ΔN* cells, NPC clustering can occur independently, as in *rat7-1* cells.

Altered interactions between NPCs and either cytoskeletal or nucleoskeletal structures could account for the NPC clustering in *rat7-1* cells. These structures could be the yeast nuclear lamina (Allen and Douglas, 1989), the nuclear envelope lattice that is thought to connect the distal rings of NPC baskets in *Xenopus laevis* (Goldberg and Allen, 1992), or cytoskeletal elements. This hypothesis predicts that Rat7p/Nup159p would be a component of one or more structures at the periphery of the NPC. For example, Rat7p/Nup159p could be a nuclear basket component involved in anchoring of the NPC to the lattice. Alternatively, Rat7p/Nup159p could be a component of either the cytoplasmic ring of the NPC or cytoplasmic filaments that emanate from the cytoplasmic face of the NPC. It is also possible that Rat7p/

Nup159p does not interact directly with these structures but could influence interactions between other NPC components and these structures.

The most unusual aspect of NPC clustering in *rat7-1* cells is the apparent restoration of nearly wild-type NPC distribution within an hour of shift to the nonpermissive temperature. This could reflect turnover of preexisting pores followed by the insertion into the nuclear envelope of new NPCs distributed normally. Alternatively, redistribution of preexisting NPCs may be occurring. Experiments are in progress to distinguish between these alternatives. Because so little is known about NPC biogenesis and turnover, it is difficult to understand the role of the mutant Rat7p in NPC distribution. Since mutant cells shifted to 37°C showed loss of mutant Rat7p from the nuclear periphery, a role for the mutant protein in NPC clustering at 23°C seems possible. This would be consistent with a gain of function for mutant Rat7p and might have been expected to be a dominant phenotype. However, NPC clustering was not seen in *RAT7/rat7-1* heterozygous diploids. Perhaps NPCs in heterozygotes contain primarily wild-type Rat7p in their NPCs. This could be due either to differences in the stability of mutant and wild-type Rat7p such that most of the Rat7p in heterozygotes might be wild-type protein or to differences in the ability of the two forms of Rat7p to become part of NPCs. NPCs are normally found clustered in some types of metazoan cells, indicating that physiological mechanisms must exist to permit NPC clustering (for examples, see Fawcett, 1981). Yeast strains with NPC clustering should be useful tools for studying NPC biogenesis and distribution.

Rat7p/Nup159p Transport Function(s)

Does Rat7p/Nup159p play a direct role in mRNA export? In a recent review about mRNA export, Elliott et al. (1994) described the type of mutant that is most likely to define a gene whose product plays a primary role in mRNA export. They suggested that a nucleoporin mutant with rapid effects on mRNA export, no rapid effect on protein import, and as few additional phenotypes as possible would be the ideal candidate. Of nucleoporin mutants characterized to date, the *rat7-1* mutant best approximates this description. In 100% of *rat7-1* cells shifted to 37°C, mRNA export was inhibited very rapidly without causing cytoplasmic accumulation of a karyophilic reporter protein. ts alleles of four other nucleoporin genes including *NUP1* (Bogerd et al., 1994), *NUP133* (Doye et al., 1994; Li et al., 1995), *NUP49* (Doye et al., 1994), and *NUP116* (Wente and Blobel, 1993) also cause nuclear retention of poly(A)$^+$ RNA, but three of these (*NUP1*, *NUP133*, and *NUP49*) require a minimum of 3 h under restrictive conditions for the phenotype to develop. Furthermore, for alleles of all three of these genes, only a fraction of the cells show accumulation of poly(A)$^+$ RNA under restrictive conditions. The slow kinetics and partial penetrance with which poly(A)$^+$ RNA accumulates in these strains makes it difficult to distinguish between primary defects in mRNA export and indirect effects resulting from impairment of other processes, such as NPC assembly or protein import. Mutant alleles of *NUP1* cause protein import defects in addition to defects in RNA export and neither defect appears rapidly following a temperature shift (Bogerd et al., 1994). In vivo repression of *NUP145* expression gradually inhibited both RNA export and protein import, but cells that accumulated nuclear poly(A)$^+$ RNA were detected several hours before cells showing cytoplasmic accumulation of a karyophilic protein (Fabre et al., 1994). The rapidly induced mRNA export block seen in *nup116Δ* cells has been shown to be an indirect consequence of membrane formation over the cytoplasmic face of nuclear pores (Wente and Blobel, 1993).

The data presented here do not eliminate the possibility that Rat7p/Nup159p also plays a direct role in protein import. First of all, in the experiment shown in Fig. 8, we do not know whether the amount of H2B-lacZ produced after the temperature shift was sufficient to permit its detection in the cytoplasm. The perfect control strain for this experiment does not exist; it would have the same rapid block in mRNA export and a rapid block in nuclear protein import. The strongest evidence that *rat7-1* cells do not have a dramatic protein import defect is the finding that normal nuclear proteins are not mislocalized in mutant cells at either 23°C or 37°C, even though modest or dramatic defects, respectively, in mRNA export were seen at these two temperatures. Even if the *rat7-1* allele shows no protein import defect, Rat7p might play a role in protein import as well as in mRNA export. Analysis of additional conditional alleles of *RAT7/NUP159* should help to clarify this possibility. Doye et al. (1994) described two ts alleles of *NUP49*; in one, the mutation affected RNA export to a much greater extent than protein import; in the other, protein import was more rapidly impaired than was RNA export.

How the RNA export defect of *rat7-1* is related to its unusual NPC clustering defect remains mysterious. Obviously, these defects could reflect two distinct properties or functions of Rat7p/Nup159p, but other explanations are also possible. Future experiments to determine where Rat7p/Nup159p localizes within the NPC and with what it interacts, both genetically and physically, should help to clarify the precise functions of the Rat7/Nup159 protein and the mechanisms underlying both cessation of mRNA export and reversible NPC clustering in *rat7* mutant cells.

We thank Louisa Howard (Rippel Microscopy Facility, Dartmouth College), C. Copeland, and P. Novick (Yale University School of Medicine) for assistance with various aspects of electron microscopy. We thank members of the Cole laboratory for discussions and advice. We thank D. Compton and B. Trumpower for critical reading of the manuscript.

These studies were supported by National Institutes of Health grant GM-33998 to C. N. Cole and National Cancer Institute core grant CA-16038 to the Norris Cotton Cancer Center. L. C. Gorsch was supported by a graduate fellowship from the Norris Cotton Cancer Center. T. C. Dockendorff was supported by training grant CA-09658 from the National Cancer Institute.

Received for publication 18 November 1994 and in revised form 3 January 1995.

References

Akey, C. W. 1989. Interactions and structure of the nuclear pore complex revealed by cryo-electron microscopy. *J. Cell Biol.* 109:955–970.

Akey, C. W., and M. Radermacher. 1993. Architecture of the *Xenopus* nuclear pore complex revealed by three-dimensional cryo-electron microscopy. *J. Cell Biol.* 122:1–19.

Allen, J. L., and M. G. Douglas. 1989. Organization of the nuclear pore complex in *Saccharomyces cerevisiae*. *J. Ultrastruct. Mol. Struct. Res.* 102: 95–108.

Altschul, S. F., W. Gish, W. Miller, M. Ew, and D. J. Lipman. 1990. Basic local alignment search tool. *J. Mol. Biol.* 215:403–410.

Amberg, D. C., A. L. Goldstein, and C. N. Cole. 1992. Isolation and character-

ization of RAT1: an essential gene of *Saccharomyces cerevisiae* required for the efficient nucleocytoplasmic trafficking of mRNA. *Genes Dev.* 6:1173–1189.

Aris, J. P., and G. Blobel. 1989. Yeast nuclear envelope proteins cross-react with an antibody against mammalian pore complex proteins. *J. Cell Biol.* 108:2059–2067.

Ausubel, F. M., R. Brent, R. E. Kingston, D. D. Moore, J. G. Seidman, and J. A. Smith. 1988. Current Protocols in Molecular Biology. John Wiley and Sons, New York.

Bogerd, A. M., J. A. Hoffman, D. C. Amberg, G. R. Fink, and L. I. Davis. 1994. *nup1* mutants exhibit pleiotropic defects in nuclear pore complex function. *J. Cell Biol.* 127:319–332.

Byers, B., and L. Goetsch. 1975. Behavior spindles and spindle plaques in the cell cycle and conjugation of *Saccharomyces cerevisiae*. *J. Bacteriol.* 124:511–523.

Carmo-Fonseca, M., H. Kern, and E. C. Hurt. 1991. Human nucleoporin p62 and the essential yeast nuclear pore protein NSP1 show sequence homology and a similar domain organization. *Eur. J. Cell Biol.* 55:17–30.

Copeland, C. S., and M. Snyder. 1993. Nuclear pore complex antigens delineate nuclear envelope dynamics in vegetative and conjugating *Saccharomyces cerevisiae*. *Yeast.* 9:235–249.

Cordes, V., I. Waizenegger, and G. Krohne. 1991. Nuclear pore complex glycoprotein p62 of *Xenopus laevis* and mouse: cDNA cloning and identification of its glycosylated region. *Eur. J. Cell Biol.* 55:31–47.

Davis, L. I., and G. Blobel. 1986. Identification and characterization of a nuclear pore complex protein. *Cell.* 45:699–709.

Davis, L. I., and G. R. Fink. 1990. The NUP1 gene encodes an essential component of the yeast nuclear pore complex. *Cell.* 61:965–978.

Doye, V., R. Wepf, and E. C. Hurt. 1994. A novel nuclear pore protein Nup133p with distinct roles in poly(A)$^+$ RNA transport and nuclear pore distribution. *EMBO (Eur. Mol. Biol. Organ.) J.* 13:6062–6075.

Dworetzky, S. I., and C. M. Feldherr. 1988. Translocation of RNA-coated gold particles through the nuclear pores of oocytes. *J. Cell Biol.* 106:575–584.

Elliott, D. J., F. Stutz, A. Lescure, and M. Rosbash. 1994. mRNA nuclear export. *Curr. Opin. Genet. Dev. Biol.* 4:305–309.

Evan, G., G. Lewis, G. Ramsay, and J. Bishop. 1985. Isolation of monoclonal antibodies specific for human *c-myc* proto-oncogene product. *Mol. Cell. Biol.* 5:3610–3616.

Fabre, E., W. C. Boelens, C. Wimmer, I. W. Mattaj, and E. C. Hurt. 1994. Nup145p is required for nuclear export of mRNA and binds homopolymeric RNA *in vitro* via a novel conserved motif. *Cell.* 78:275–289.

Fawcett, D. 1981. The Cell. W. B. Saunders Co., Philadelphia.

Gerace, L. 1992. Molecular trafficking across the nuclear pore complex. *Curr. Opin. Cell Biol.* 4:637–645.

Gietz, R. D., and A. Sugino. 1988. New yeast-*Escherischia coli* shuttle vectors constructed with *in vitro* mutagenized yeast genes lacking six-base pair restriction sites. *Gene.* 74:527–534.

Goldberg, M. W., and T. D. Allen. 1992. High resolution scanning electron microscopy of the nuclear envelope: the baskets of the nucleoplasmic face of the nuclear pores. *J. Cell Biol.* 119:1429–1440.

Grandi, P., V. Doye, and E. C. Hurt. 1993. Purification of NSP1 reveals complex formation with 'GLFG' nucleoporins and a novel nuclear pore protein NIC96. *EMBO (Eur. Mol. Biol. Organ.) J.* 12:3061–3071.

Guthrie, C., and G. R. Fink. 1991. Guide to yeast genetics and molecular biology. *Methods Enzymol.* 194:423–424.

Hallberg, E., R. W. Wozniak, and G. Blobel. 1993. An integral membrane protein of the pore membrane domain of the nuclear envelope contains a nucleoporin-like region. *J. Cell Biol.* 122:513–521.

Hinshaw, J. E., B. O. Carragher, and R. A. Milligan. 1992. Architecture and design of the nuclear pore complex. *Cell.* 69:1133–1141.

Huang, S., T. J. Deerinck, M. H. Ellisman, and D. L. Spector. 1994. In vivo analysis of the stability and transport of nuclear poly(A)$^+$ RNA. *J. Cell Biol.* 126:877–899.

Hurt, E. C. 1988. A novel nucleoskeletal-like protein located at the nuclear periphery is required for the life cycle of *Saccharomyces cerevisiae*. *EMBO (Eur. Mol. Biol. Organ.) J.* 7:4323–4334.

Izzauralde, E., and I. W. Mattaj. 1992. Transport of RNA between nucleus and cytoplasm. *Semin. Cell Biol.* 3:279–288.

Jarnik, M., and U. Aebi. 1991. Toward a more complete 3-D structure of the nuclear pore complex. *J. Struct. Biol.* 107:291–308.

Li, O., C. V. Heath, D. C. Amberg, T. C. Dockendorff, C. Copeland, M. Snyder, and C. N. Cole. 1995. Mutation or deletion of the *Saccharomyces cerevisiae RAT3/NUP133* gene causes temperature-dependent nuclear accumulation of poly(A)$^+$ RNA and constitutive clustering of nuclear pore complexes. *Mol. Biol. Cell.* 6:401–417.

Loeb, J., L. I. Davis, and G. R. Fink. 1993. NUP2, a novel yeast nucleoporin, has functional overlap with other proteins of the nuclear pore complex. *Mol. Biol. Cell.* 4:209–222.

Lupas, A., M. Van Dyke, and J. Stock. 1991. Predicting coiled coils from protein sequences. *Science (Wash. DC).* 252:1162–1164.

Maquat, L. E. 1991. Nuclear mRNA export. *Curr. Biol.* 3:1004–1012.

Maul, G. G. 1977. The nuclear and cytoplasmic pore complex: structure, dynamics, distribution and evolution. *Int. Rev. Cytol.* 6(Suppl):75–186.

Mehlin, H., B. Daneholt, and U. Skoglund. 1992. Translocation of a specific premessenger ribonucleoprotein particle through the nuclear pore studied with electron microscope tomography. *Cell.* 69:605–613.

Moreland, R., G. Langevin, R. Singer, R. Garcea, and L. Hereford. 1987. Amino acid sequences that determine the nuclear localization of yeast histone 2B. *Mol. Cell. Biol.* 7:4048–4057.

Mutvei, A., S. Dihlmann, W. Herth, and E. C. Hurt. 1992. NSP1 depletion in yeast affects nuclear pore formation and nuclear accumulation. *Eur. J. Cell Biol.* 59:280–295.

Nehrbass, U., H. Kern, A. Mutvei, H. Horstmann, B. Marshallsay, and E. C. Hurt. 1990. NSP1: a yeast nuclear envelope protein localized at the nuclear pores exerts its essential function by its carboxy-terminal domain. *Cell.* 61:979–989.

Pearson, W. 1994. Using the FASTA program to search protein and DNA sequence databases. *Methods Mol. Biol.* 25:365–389.

Reichelt, R., A. Holzenburg, E. L. Buhle, Jr., M. Jarnik, A. Engel, and U. Aebi. 1990. Correlation between structure and mass distribution of the nuclear pore complex and of distinct pore complex components. *J. Cell Biol.* 110:883–894.

Ris, H. 1991. The three-dimensional structure of the nuclear pore complex as seen by high voltage electron microscopy and high resolution low voltage scanning electron microscopy. *EMSA Bull.* 21:54–56.

Rose, M. D., F. Winston, and P. Hieter. 1989. Methods In Yeast Genetics. Cold Spring Harbor Laboratory, Cold Spring Harbor, NY.

Rout, M., and G. Blobel. 1993. Isolation of the yeast nuclear pore complex. *J. Cell Biol.* 123:771–783.

Rout, M., and S. Wente. 1994. Pores for thought: nuclear pore complex proteins. *Trends Cell Biol.* 4:357–365.

Sanger, F., S. Nicklen, and A. R. Coulson. 1977. DNA sequencing with chain terminating inhibitors. *Proc. Natl. Acad. Sci. USA.* 74:5463–5467.

Scheer, U., M. Dabauvalle, H. Merkert, and R. Benevente. 1988. The nuclear envelope and the organization of the pore complexes. *Cell Biol. Int. Rep.* 12:669–689.

Silver, P. A. 1991. How proteins enter the nucleus. *Cell.* 64:489–497.

Snow, C. M., A. Senior, and L. Gerace. 1987. Monoclonal antibodies identify a group of nuclear pore complex glycoproteins. *J. Cell Biol.* 104:1143–1156.

Spurr, A. R. 1969. A low-viscosity resin embedding medium for electron microscopy. *Journal of Ultrastructure Research.* 26:31–43.

Starr, C. M., M. D'Onofrio, M. K. Park, and J. A. Hanover. 1990. Primary sequence and heterologous expression of nuclear pore glycoprotein p62. *J. Cell Biol.* 110:1861–1871.

Stevens, B. J., and H. Swift. 1966. RNA transport from nucleus to cytoplasm in *Chironomus* salivary glands. *J. Cell Biol.* 31:55–77.

Stewart, M., and S. Whytock. 1988. The structures and interactions of components of nuclear envelopes from *Xenopus* oocyte germinal vesicles observed by heavy metal shadowing. *J. Cell Sci.* 90:409–423.

Sukegawa, J., and G. Blobel. 1993. A nuclear pore complex protein that contains zinc finger motifs, binds DNA, and faces the nucleoplasm. *Cell.* 72:29–38.

Unwin, P. N., and R. A. Milligan. 1982. A large particle associated with the perimeter of the nuclear pore complex. *J. Cell Biol.* 93:63–75.

Wente, S., and G. Blobel. 1994. NUP145 encodes a novel yeast glycine-leucine-phenylalanine-glycine (GLFG) nucleoporin required for nuclear envelope structure. *J. Cell Biol.* 125:955–969.

Wente, S. R., and G. Blobel. 1993. A temperature-sensitive NUP116 null mutant forms a nuclear envelope seal over the yeast nuclear pore complex thereby blocking nucleocytoplasmic traffic. *J. Cell Biol.* 123:275–284.

Wente, S. R., M. P. Rout, and G. Blobel. 1992. A new family of yeast nuclear pore complex proteins. *J. Cell Biol.* 119:705–723.

Wimmer, C., V. Doye, P. Grandi, U. Nehrbass, and E. C. Hurt. 1992. A new subclass of nucleoporins that functionally interact with nuclear pore protein NSP1. *EMBO (Eur. Mol. Biol. Organ.) J.* 11:5051–5061.

Wozniak, R. W., G. Blobel, and M. P. Rout. 1994. POM152 is an integral protein of the pore membrane domain of the yeast nuclear envelope. *J. Cell Biol.* 125:31–42.

Wright, R., and J. Rine. 1989. Transmission electron microscopy and immunocytochemical studies of yeast: analysis of HMG-CoA reductase overproduction by electron microscopy. *Methods Cell Biol.* 31:473–512.

Yano, R., M. Oakes, M. Yamaghishi, J. A. Dodd, and M. Nomura. 1992. Cloning and characterization of SRP1, a suppressor of temperature-sensitive RNA polymerase I mutations, in *Saccharomyces cerevisiae*. *Mol. Cell. Biol.* 12:5640–5651.